

UNCLASSIFIED

AD NUMBER
AD920469
NEW LIMITATION CHANGE
TO Approved for public release, distribution unlimited
FROM Distribution authorized to U.S. Gov't. agencies only; Administrative/Operational Use; May 1974. Other requests shall be referred to Rome Air Development Center, Griffis AFB, NY.
AUTHORITY
RADC, usaf ltr, 12 aug 1976

THIS PAGE IS UNCLASSIFIED

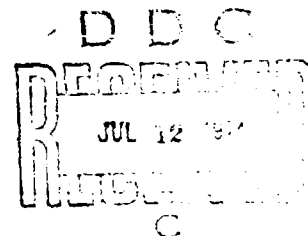
RADC-TR-74-111
Final Report
May 1974



AD920469

CHEMICAL REACTION HERTZIAN GENERATOR

Braddock, Dunn and McDonald, Inc.



*Distribution limited to U. S. Government agencies only;
Test and Evaluation; May 1974. Other requests for this
document must be referred to RADC/OCTP, Griffiss AFB,
NY 13441.*

Rome Air Development Center
Air Force Systems Command
Griffiss Air Force Base, New York

CHEMICAL REACTION HERTZIAN GENERATOR

Dr. K. S. Kunz
Braddock, Dunn and McDonald, Inc.

Distribution limited to U. S. Government agencies only; Test and Evaluation; May 1974. Other requests for this document must be referred to RADC/OCTP, Griffiss AFB, NY 13441.

Do not return this copy. Retain or destroy.

FOREWORD

This report was prepared by Braddock, Dunn and McDonald, Inc., 5301 Central Avenue NE, Suite 1717, Albuquerque, NM 87108 as part of study contract F30602-73-C-0318, Job Order No. 55730644, extending from 31 May to 31 December 1973. The BDM report number is BDM/A-1-74-TR.

Mr. William Quinn has served as the RADC technical coordinator, providing important guidance throughout the study. BDM contributors to the report were Mr. D. T. Bailey, Mr. T. H. Lehman, Dr. K. S. Kunz, and Dr. J. S. Yu.

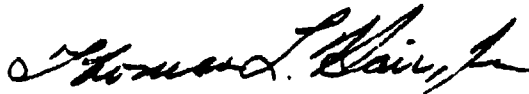
This report has been reviewed and is approved.

APPROVED:



WILLIAM C. QUINN
RADC Project Engineer

APPROVED:



THOMAS L. HAIR, Jr.
Colonel, USAF
Chief, Surveillance and Control Division

FOR THE COMMANDER:



CARLO P. CROCETTI
Chief, Plans Office

ABSTRACT

This effort represents a first attempt at combining the two separate technologies of explosive flux compression and Hertzian generation for the purpose of obtaining ultra-high energy pulses at microwave frequencies. A number of interesting concepts were analyzed and three were selected by the contractor as most deserving of future attention. It is hoped that this report will stimulate further imaginative and creative thought in this direction leading eventually to a successful technique for accomplishing the aforementioned goal.

TABLE OF CONTENTS

<u>Section</u>	<u>Page</u>
I INTRODUCTION	1-1
1. BACKGROUND	1-2
a. Superior Storage Capabilities of Chemical Sources	1-2
b. Availability of High Energy Explosive Flux Compression Generators	1-2
2. MICROWAVE PRODUCTION FROM A CHEMICAL SOURCE	1-5
a. Rationale	1-5
b. RADC Requirements	1-6
3. UNSUITABILITY OF CHEMICAL GENERATOR ALONE	1-6
a. Device Configuration	1-6
b. Spectral Output at 1 GHz	1-8
c. Conclusions	1-14
II STUDY	11-1
1. GENERAL DISCUSSION	11-1
a. Purpose of Study	11-1
b. Representative Solutions	11-1
2. STUDY APPROACH	11-3
a. Literature Survey	11-3
b. Conceptual Design and Analysis	11-4
c. In-Depth Analysis	11-4
d. Documentation	11-4
3. SUMMARY STATEMENT	11-5
III DEVICES DESIGNED AND ANALYZED	111-1
1. FROZEN E-FIELD DEVICE	111-1
a. Configuration	111-1
b. Principle of Operation	111-1
c. Traveling Wave Decomposition	111-2
d. Further Operational Details	111-3
e. Design Considerations	111-3
f. Conclusions	111-7
2. FROZEN B-FIELD DEVICES	111-8
a. Slotted Frozen B-Field Device	111-8
b. Coaxial Frozen B-Field Device	111-18
c. Frozen B-Field Devices: General Switching Considerations	111-33

TABLE OF CONTENTS (Continued)

<u>Section</u>	<u>Page</u>
3. FERROELECTRIC DEVICE	111-36
a. Introduction	111-36
b. Energy Storage Capabilities	111-37
c. Transition	111-38
d. Switching Times	111-38
e. Simultaneity	111-40
f. Coupling of the Ferroelectric Device to an Antenna	111-42
4. MOVING MIRROR APPROACHES	111-46
a. Introduction	111-46
b. Single Reflection	111-46
c. Multiple Reflections	111-47
5. PLASMA OSCILLATIONS	111-51
6. CAPACITIVE DISCHARGE APPROACH	111-53
7. SYNCHROTRON RADIATION	111-55
8. BRILLOUIN AND RAMAN SCATTERING	111-57
9. CANDIDATE RANKINGS	111-58
IV MODIFIED DESIGN REQUIREMENTS	IV-1
1. BREAKDOWN CONSIDERATIONS	IV-1
a. General Discussion	IV-1
b. Inside the Frozen E- and B-Devices	IV-2
c. Outside Any Device	IV-3
2. ANTENNA SIZE AND POWER CAPABILITIES	IV-5
3. MODIFIED DESIGN REQUIREMENTS	IV-6
V IN-DEPTH ANALYSIS	V-1
1. FROZEN E-FIELD DEVICE	V-1
a. Assumptions	V-1
b. Admissibility of a 1 cm Gap	V-1
c. Internal Electric Field Strength	V-2
d. Device Size as Required by Switch Closure Times	V-2
e. Energy Storage Capabilities	V-4
f. Configuration	V-5
2. FROZEN B-FIELD DEVICE	V-6
a. Remote Switches	V-6
b. Multiple Switches	V-10

TABLE OF CONTENTS (Continued)

<u>Section</u>	<u>Page</u>
3. FERROELECTRIC DEVICE	V-14
a. Attenuation Loss Solution	V-14
b. Coupling Problems	V-15
VI CONCLUSIONS AND RECOMMENDATIONS	VI-1
1. CONCLUSIONS	VI-1
2. RECOMMENDATIONS	VI-5
REFERENCES	VI-7
BIBLIOGRAPHY	VI-9
APPENDIX A	A-1
APPENDIX B	B-1
APPENDIX C	C-1
APPENDIX D	D-1

EVALUATION

Project:
Contract No:
Effort Title:

5573
F30602-73-C-0318
CHEMICAL REACTION
HERTZIAN GENERATOR

Contractor:

Braddock, Dunn & McDonald
1st National Bank Bldg
Albuquerque, NM 87108

Hertzian generators in general exhibit simple, reliable, low cost, microwave capability at high power and very short pulse duration (eg. ten rf cycles). Explosive flux compression technology over the past few years has demonstrated megagauss and megampere outputs in relatively simple, reliable, low cost devices. A marriage of the two technologies for the purpose of generating intense bursts of microwave energy appears inevitable. This effort represents a first step in this direction.

All known conceivable technical schemes were analyzed, even if somewhat briefly, and categorized according to probable probability of success. Three approaches were selected by the contractor as being worthy of further consideration. At this point it is probably wise to keep an open mind i.e. it is entirely possible that modifications to remove the objectionable aspects of any of the schemes studied could lead to a practical device.

This effort is part of RADC Technology Plan TP05.


WILLIAM C. QUINN
RADC/OCTP

CHEMICAL REACTION HERTZIAN GENERATOR FINAL REPORT

SECTION I

INTRODUCTION

Chemical reactions can release large amounts of energy from a given mass in comparison to conventional storage devices such as capacitors. Explosives have been used in magnetic flux compression devices to convert a part of this chemical energy into megagauss fields with an energy content above 1 MJ. The ability to convert an appreciable fraction of the electromagnetic energy stored in this field into a radiating field at microwave frequencies would result in a compact, high power source of microwave energy. Currently available devices of this type cannot convert a significant amount of the stored energy into microwave radiation; other methods are needed to obtain significant microwave output. For this reason then, a study was initiated by the Rome Air Development Center to establish the feasibility of obtaining appreciable microwave energy from a chemical source by alternate methods. Among the methods identified for analysis were "frozen wave" devices, moving mirror techniques, and the explosive depolarization of a ferroelectric.

The remainder of this section contains a background.

Section II is a synopsis of study conducted. Representative solutions are presented along with the study approach. The section ends with a summary statement about the results of the study.

The detailed technical analysis follows. Section III contains a preliminary analysis of the devices that were considered as possibilities. In Section IV, modifications to the Rome Air Development Center design requirements are made. This was done because of electrical breakdown limitations. Those devices in Section III found promising are analyzed in greater depth in Section V. Device capabilities are determined for specific design configurations.

The report concludes with Section VI, CONCLUSIONS AND RECOMMENDATIONS.

1. BACKGROUND

a. Superior Storage Capabilities of Chemical Sources

A chemical source of energy such as TNT provides a very large amount of energy from a very compact source of light weight in comparison to conventional electric storage devices such as a capacitor bank. This point can be illustrated more explicitly by considering the mass required to store one megajoule of energy in various storage devices. The nominal figures are:

(1) 10^4 kg - high performance capacitor bank

(2) 2kg - battery

(3) 2×10^{-7} kg - TNT

b. Availability of High Energy Explosive Flux Compression Generators

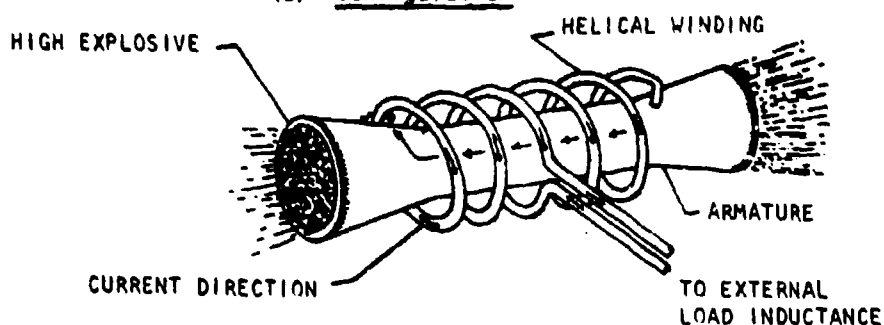
At the present time, numerous groups have produced and are experimenting with explosive flux compression generators. They include Sandia Laboratories, Los Alamos Scientific Laboratories, and the Frascati Institute in Italy.

Typically, the devices in use at these laboratories use explosives to compress a small initial magnetic field inside a cylinder of high permeability and conductivity material (stainless steel, for example). This in turn, in some of the designs, has produced field strengths as high as 5 megagauss or more with an energy content of as much as several megajoules. In some of the devices, the Sandia generators in particular, this energy is used to produce an intense current of several mega-amperes.

Two devices, one from Sandia and one from Los Alamos, are fairly representative and their configuration and performance is discussed below.

(1) Sandia Type 169 Generator

(a) Configuration



(b) Principle of Operation

Reference (1) describes the device's operation as follows:

"A starting current, I_0 (injected by a capacitor bank), produces a magnetic field between the coil and the armature; the armature is then expanded by detonating the explosive simultaneously at both ends. The emf resulting from the armature motion

causes the current in the generator to increase and, under normal conditions, the current will continue to increase until the armature reaches the connection point to the external load inductance. At this point, the generator has completed its operation, the result being that a current of several mega-amperes has been delivered to the load."

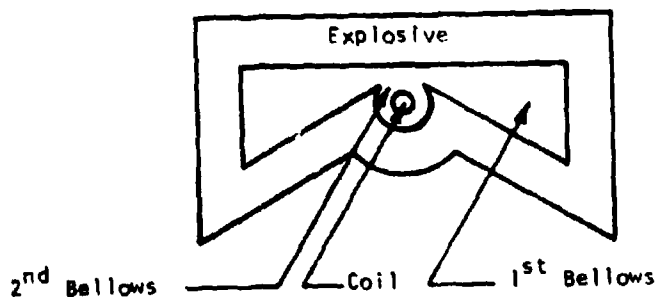
(c) Performance Parameters

- (1) Risetime (10% - 90%) - 45 usec
- (2) Current peak - 6.5 - 7.0 MA
- (3) Energy delivered - 1.5 MJ
- (4) Explosive weight - 17 lbs
- (5) Efficiency - 4%
- (6) $di/dt - > 4.0 \times 10^{12}$ A/sec

(2) Los Alamos Generator

(a) Configuration

Dual bellows arrangement with coil pickup in second bellows.



(b) Principle of Operation

Two stage explosive magnetic flux compression. Pickup coil converts time varying field into output current.

(c) Performance Parameters

- (1) Risetime (10% - 90%) - 3 μ s
- (2) Voltage Output - 10^5 volts (~ constant voltage source)
- (3) Current Capabilities - kiloampere range for loads used at LASL, ~ 13 μ H.

2. MICROWAVE PRODUCTION FROM A CHEMICAL SOURCE

a. Rationale

A chemical generator takes the stored energy of a high explosive and releases it by detonating this explosive. A portion of this energy is used to impart kinetic energy to the "liner" which in turn compresses the initial field. This yields a higher field strength and, hence, higher energy content of the field. The energy in the field is obtained from the kinetic energy of the liner which is doing work in compressing the field.

While fairly inefficient, an efficiency of a few percent in practice, the large chemical energy in the explosives is enough to result in as much as 1 MJ or more energy, stored in the electromagnetic field. If the electromagnetic energy or an appreciable fraction of it, could be made to take the form of a radiating field in the microwave region, a compact, extremely high power source of microwave energy would be made available.

b. RADC Requirements

For this study feasibility was to be determined with respect to a set of criteria established by the Rome Air Development Center (RADC). A device meeting these criteria would be an extremely powerful, compact source of microwave energy. The criteria are:

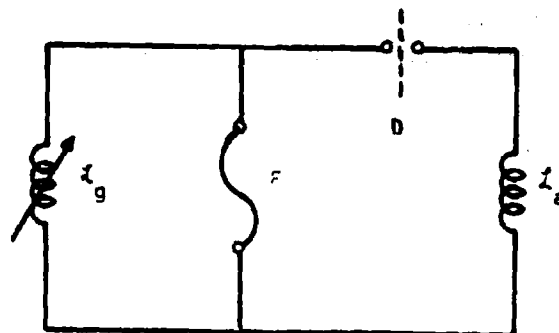
- (1) Power $\geq 10^{12}$ watts.
- (2) Frequency ≥ 1 GHz.
- (3) Pulse Duration ≥ 10 cycles.
- (4) Portable - for example, could be aircraft borne.
- (5) Repetition Rate - single shot to one pulse per second.
- (6) Implied Requirement, Energy Content - requirements (1), (2), and (3) imply an energy content $\approx 10^4$ joules.

3. UNSUITABILITY OF CHEMICAL GENERATOR ALONE

a. Device Configuration

A Sandia type generator of nominal characteristics is used to feed a single loop antenna. This device configuration is characteristic of the methods that could be used to obtain microwave energy directly from a chemical generator. Other generator types could be employed, but the results would be similar. Nominal values for the device performance will be employed and it will be assumed that the antenna load is well matched to the generator.

This configuration, both without and with an idealized peaking circuit, and with the pulse "chopped" into half a square wave is examined. The peaking circuit is designed to transfer the current output from a primary path to a secondary path. Treating the generator as a time varying inductance, and the antenna as an inductive load, this can be represented as



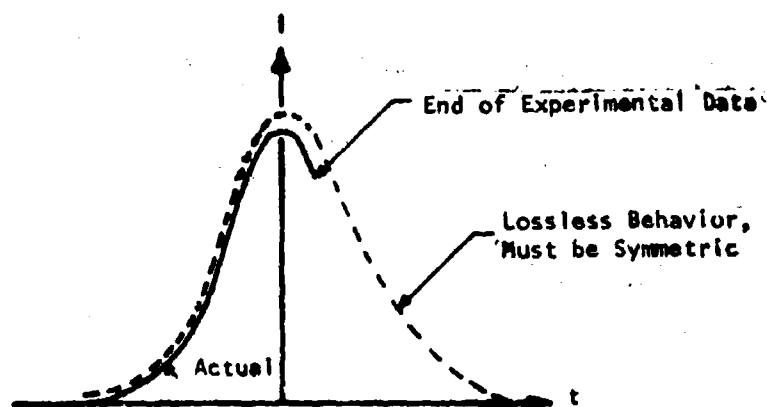
where Z_g is the generator inductance, Z_a the antenna inductance, F is a fast blow fuse that sends a voltage pulse out that triggers D , a dielectric switch, transferring the current from the primary path with the fuse to the secondary path with the antenna.

The effect of the peaking circuit, if properly timed, is to chop the current output to the antenna so that instead of the antenna seeing the slow current buildup characteristic of the chemical generator, it receives a current that quickly rises to the peak current value, then decays as before. Real values for the risetime with a peaking circuit are on the order of 1 μsec as opposed to the 10 μsec characteristic of the generator itself. An idealized peaking circuit would have zero risetime and would affect the transfer at the moment of maximum current flow through the primary side.

b. Spectral Output at 1 GHz

(1) Without Peaking Circuit

A nominal chemical generator will have a 10 μsec risetime (10 percent - 90 percent) to reach a current peak of 5×10^6 amps into an inductive load of ~ 80 nH with a resulting energy maximum of $E = \frac{1}{2} L I^2 = 1.00 \times 10^6$ joules. The current growth is exponential for most of the growth period. The overall time behavior, graphically displayed, is



Treating the idealized lossless time behavior, the energy of the fields inside the device as a function of time is

$$g(t) = U_0 \operatorname{sech} \frac{t}{T_0} = U_0 \frac{2}{e^{(t/T_0)} + e^{-(t/T_0)}},$$

where U_0 is the maximum energy of the field and $T_0 = 2.17 \mu\text{sec}$, T_0 is determined from the fact that the energy increases by a factor of 81 in 10 μsec .

Fourier analyzing $g(t)$ yields

$$g(t) = \frac{1}{2\pi} \int_{-\infty}^{\infty} G(\omega) e^{j\omega t} d\omega$$

where $G(\omega) = U_0 T_0 \operatorname{sech} \frac{\omega T_0}{2}$.

The largest component is at $\omega = 0$. At 1 GHz, the ratio of amplitudes, R , is

$$\begin{aligned} R &= \frac{\operatorname{sech}(\omega T_0/2)}{\operatorname{sech} 0} \\ &= \frac{\operatorname{sech} \pi \cdot 10^9 \operatorname{sech}^{-1} \times 1.7 \times 10^{-6} \operatorname{sech}}{1} \\ &= \operatorname{sech} 0.68 \times 10^4 \\ &= \frac{2}{e^{0.68 \times 10^4} + e^{-0.68 \times 10^4}} \end{aligned}$$

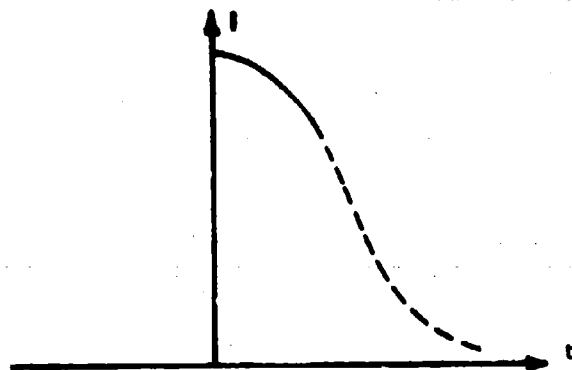
Therefore,

$$R \approx 2 \times e^{-0.68 \times 10^4} = 2 \times 10^{-2,940}$$

and the energy content at 1 GHz is insignificant.

(2) With Idealized Peaking Circuit

An idealized peaking circuit, properly timed so that the current peak is transferred to the secondary side instantly, yields a current through the antenna that looks like the following:



The energy time behavior can be described by

$$f(t) = g(t) u(t)$$

where $g(t)$ is the same time behavior as given for the configuration without the peaking circuit and $u(t)$ is the Heaviside function.

The Fourier transform is

$$\begin{aligned} G(\omega) &= \frac{1}{2\pi} \int_0^{\infty} g(t) e^{-i\omega t} d\omega \\ &= \frac{1}{2\pi} \int_0^{\infty} U_0 \operatorname{sech} \left(\frac{t}{T_0} \right) e^{-i\omega t} d\omega \\ &= \frac{U_0 T_0}{2\pi} \beta \left(\frac{1 - i\omega T_0}{2} \right) \\ &= \frac{U_0 T_0}{4\pi} \left[\psi \left(\frac{3 - i\omega T_0}{4} \right) - \psi \left(\frac{1 - i\omega T_0}{4} \right) \right] \end{aligned}$$

where β is the incomplete beta function and ψ is Euler's psi function

For large arguments $\psi(x) \approx \frac{1}{2x}$

$$G(\omega) \approx \frac{U_o T_o}{8\pi} \left[\frac{4}{3 - j\omega T_o} - \frac{4}{1 - j\omega T_o} \right]$$

$$\approx \frac{U_o T_o}{\pi} \frac{1}{(\omega T_o)^2}$$

While for $\omega = 0$

$$G(0) = \frac{U_o T_o}{4}$$

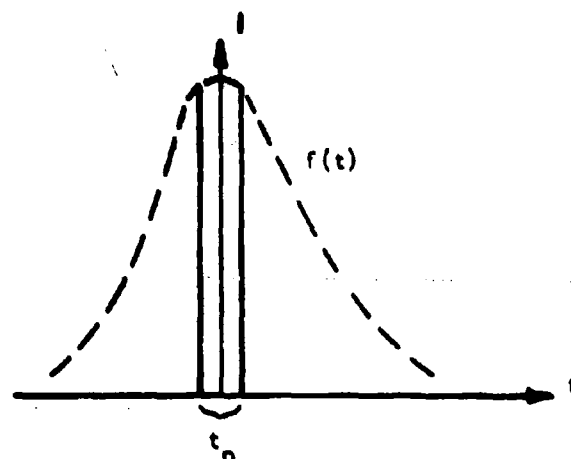
The ratio, R, of $G(\omega = 2\pi \times 10^9)$ to $G(0)$ is

$$R = \frac{G(2\pi \times 10^9)}{G(0)} = \frac{1}{\pi(\omega T_o)^2} \approx \frac{1}{4\pi \times 10^8}$$

This is a considerable improvement over the unpeaked output, but still represents insignificant 1 GHz output.

(3) Output "Chopped" to Look Like a Half Square Wave

If the idealized peaking circuit were augmented with an infinitely fast opening switch in series with the dielectric switch on the secondary side, then the current to the antenna could be made to resemble a half square wave, that is



Parsival's theorem states that the energy represented in this square pulse with respect to the energy of the whole pulse is given by the ratio R, where

$$R = \frac{\int_{-t_0/2}^{t_0/2} f(t) dt}{\int_{-\infty}^{\infty} f(t) dt}$$

$$= \frac{\left[\int_{-t_0/2}^{t_0/2} \text{sech} \left(\frac{t}{T_0} \right) dt \right]}{\left[\int_{-\infty}^{\infty} \text{sech} \left(\frac{t}{T_0} \right) dt \right]}$$

$$= \frac{\tan^{-1} \left(\sinh \left(\frac{t}{T_0} \right) \right) \Big|_{-t_0/2}^{t_0/2}}{\tan^{-1} \left(\sinh \left(\frac{t}{T_0} \right) \right) \Big|_{-\infty}^{\infty}}$$

$$= \frac{t_0}{\pi T_0} \text{ for } t_0 \ll T_0.$$

The Fourier decomposition of a square wave yields

$$F(\omega) = \frac{\sin(\omega t_0/2)}{(\omega t_0/2)}.$$

If the spectrum is not to fall off at $\omega = 2\pi \times 10^9$, t_0 must be less than 10^{-9} sec. For $t_0 = \frac{1}{2}$ ns

$$\begin{aligned} R &= \frac{\frac{1}{2} \times 10^{-9}}{\pi \cdot 2.17 \times 10^{-6}} \\ &= 0.734 \times 10^{-4}. \end{aligned}$$

If the whole pulse contained 10^6 joules, a typical value, then the square pulse contains 73.4 joules. Further, only a fraction of this energy is in the spectral region about 1 GHz. In particular, this fraction is given for the frequency band of 1 GHz to 2 GHz by

$$\begin{aligned} & \frac{2 \int_{2\pi \times 10^9}^{4\pi \times 10^9} F(\omega) d\omega}{\int_{-\infty}^{\infty} F(\omega) d\omega} \\ &= 2 \frac{\int_{2\pi \times 10^9}^{4\pi \times 10^9} \frac{\sin(\omega t_0/2)}{(\omega t_0/2)} d\omega}{\int_{-\infty}^{\infty} \frac{\sin(\omega t_0/2)}{(\omega t_0/2)} d\omega} \end{aligned}$$

$$= \frac{2 \left(\frac{2}{t_0} \right) \text{Si} \left(\frac{\omega t_0}{2} \right) \Big|_{2\pi \times 10^9}^{4\pi \times 10^9}}{2\pi/t_0}$$

$$= \frac{\text{Si}(2\pi) - \text{Si}(\pi)}{\pi/2} \approx \frac{1}{4}$$

where Si is the sin integral. As a result only ~ 18 Joules from 1 - 2 GHz is produced.

c. Conclusions

It can be concluded that the spectral output of the chemical generator by itself, without peaking circuits, is effectively zero about 1 GHz. Nor does a peaking circuit help sufficiently. The same is true for chopping the output to form a square pulse. Other methods must be employed to obtain the desired output of 10^4 joules in the vicinity of 1 GHz.

SECTION II

STUDY

1. GENERAL DISCUSSION

a. Purpose of Study

The fact that the currently available chemical generators cannot produce significant output at microwave frequencies motivated this study. The purpose of the study was to find methods of converting the high energy output of chemical generators to the required frequency while maintaining a significant energy level as well as to explore novel chemical generator concepts that might directly produce a high energy 1 GHz output.

b. Representative Solutions

(1) Intermediate Device for Frequency Conversion

One broad approach to obtaining high frequencies and energies is to treat the chemical generator as a source of electrical energy that can be stored in an intermediate device. This intermediate device can be composed of storage elements of one-half wavelength at 1 GHz. In this fashion, the intermediate device is "tuned" to a 1 GHz resonance. Fast acting switches release the stored energy from the device and it will radiate most strongly at 1 GHz.

An example of this approach is the frozen E-field device. It consists of a segmented transmission line in which electrical energy is stored capacitively in alternating polarity from segment to segment. A detailed treatment of this device can be found in Reference (2). Graphically, it looks like



The gaps between segments can be closed using a spark gap arrangement. The stored energy is then allowed to propagate. Provided the switches are fast enough not to degrade the waveform, the square waveform will be preserved. If the device is air filled and the segments are of length 15 cm, the first harmonic¹ of this waveform will be at 1 GHz.

Two general features of this approach are

- (1) Resonant elements.
- (2) Nonlinear operation (i.e., switching).

The first feature determines the frequency of operation. The second allows the frequency conversion to take place. Any device using only linear elements will not result in frequency conversion. For a conventional chemical generator using an intermediate device to produce enhanced output at 1 GHz, the intermediate device must employ nonlinear elements. Further, as seen in Section 1, the use of a nonlinear device alone, in this case to peak the current output, does not provide sufficient frequency conversion.

(2) Novel Devices

An example of a novel approach is what will be called the ferroelectric device in a later section. The basic feature of interest for this device is the use of very thin sheets of BaTiO_3 , a ferroelectric.

¹ See Appendix D for the formal definition of the first harmonic.

They are assumed to be polarized. The energy in the polarized field can be released by the use of explosive to depolarize the material. The very thinness of the sheets ($\sim 6 \times 10^{-4}$ cm), and the explosive velocities involved ($\sim .3 - .5$ cm/ μ sec), insure that the process will take place in approximately 1 ns.

It is the very short time of operation that allows the system to produce appreciable energy at 1 GHz. In effect, the dimensions of a conventional generator are scaled down sufficiently, while the explosive velocities remain constant, yielding a very fast peaking pulse. A Fourier decomposition of such a pulse, just as for the half square wave, yields appreciable output about 1 GHz if the pulse peaks quickly enough. This approach is considered novel in that a variation in generator configuration is used instead of an intermediate device.

2. STUDY APPROACH

The study was conducted in four stages as discussed below.

a. Literature Survey

This provided:

- (1) Theoretical background.
- (2) Design parameters of various concepts.
- (3) Novel approaches.
- (4) Extensive bibliography.

b. Conceptual Design and Analysis

The work performed at this stage consisted of:

- (1) Cataloging possible devices.
- (2) Preliminary device evaluation.
- (3) Selection of most promising device types.

c. In-Depth Analysis

This last technical stage was an in-depth study of the promising devices. It provided:

- (1) Formulation of general design restrictions.
- (2) Modified design requirements arising from design restrictions.
- (3) Detailed model configuration of promising device types.
- (4) In-depth analysis of these detailed configurations.

d. Documentation

This report constitutes the documentation of this study. It contains:

- (1) Devices designed and analyzed.
- (2) Modified design requirements.

(3) In-depth analysis of promising device types.

(4) Conclusions and recommendations.

(5) Bibliography.

3. SUMMARY STATEMENT

The results and conclusions of this study can be briefly summarized here. The technical basis for these statements is contained in the subsequent sections on devices designed and analyzed and in-depth analyses of promising devices. More detailed conclusions and recommendations are contained in the final section on conclusions and recommendations.

In summary:

- (1) Only 10^{10} watts or less at 1 GHz can be delivered from a 1 m^2 aperture antenna at altitudes of $\sim 5 \text{ km}$ or greater because of breakdown phenomena.
- (2) A frozen E-field device using SF_6 at 100 atmospheres and 1 cm gaps fired by a UV laser can store 460 joules of energy, delivering up to 230 joules at 1 GHz for a power level of 2.3×10^{10} watts.
- (3) Storage volume dimensions, $150 \text{ cm} \times 1/2 \text{ cm} \times 2.6 \text{ cm}$, and jitter as low as 0.1 ns, allow the use of multiple E-field devices working in parallel to produce much higher energy output.
- (4) Other promising device types, the coaxial frozen B-field device and the ferroelectric device, have lower efficiency and storage capacity along with switching difficulties and fabrication problems respectively.

- (5) Further investigation of the power limitations set by breakdown phenomena at altitudes above ~ 5 km are needed to more accurately set these limitations.
- (6) Further investigation of nonlinear devices and novel devices is needed. Only a fraction of the possibilities that might be feasible have been examined in the relatively short time span of this report.

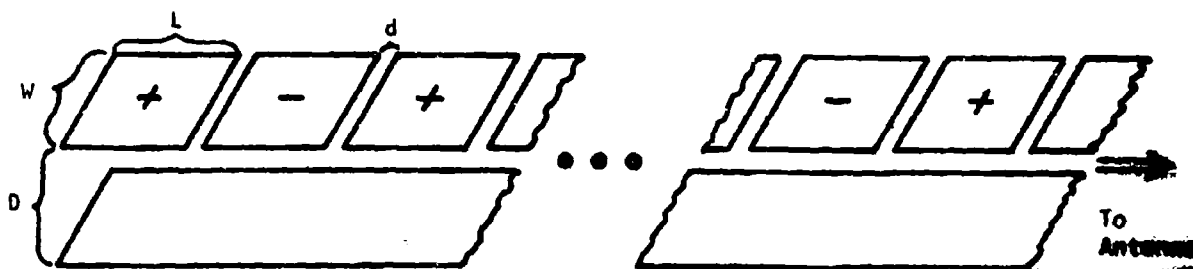
SECTION III

DEVICES DESIGNED AND ANALYZED

1. FROZEN E-FIELD DEVICE

a. Configuration

The frozen E-field device under consideration is configured as a segmented transmission line as follows.



The upper plate is segmented into 10 elements with a separation or gap d . Each plate is of length L , width W , and is separated from the bottom strip by distance D .

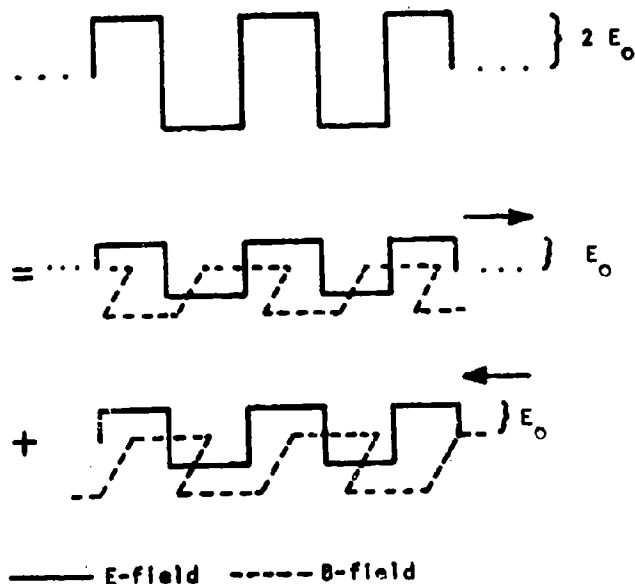
b. Principle of Operation

Alternate plates are oppositely charged establishing a static E-field that is approximately represented spatially by a square wave with periodicity $2L$ and amplitude $2E_0$. Switches, typically spark gaps for fast switching times and high power capacity, are used to simultaneously short the plate elements together. The charge is no longer constrained, allowing

current flow, thereby supporting a now propagating electromagnetic field. This is referred to as "unfreezing" the "frozen" field. The device now acts as a transmission line allowing all of the stored energy to propagate. A more detailed analysis of the analogous process for a frozen B-field device is contained in Section III. 2, a (2).

c. Traveling Wave Decomposition

The propagating field can be represented by two square waves of amplitude E_0 and period $2L$ traveling in opposite directions down the transmission line. These two waves at $t = 0$, when the device is switched, must have identical spatial distribution of their E-field, so that their superposition yields the frozen E-field distribution. The B-fields associated with each traveling wave exactly cancel at this time, since each is in quadrature with identical E-fields; only one is $\pi/2$ advanced and the other $\pi/2$ retarded. This is illustrated as follows:



d. Further Operational Details

One end of the strip line is loaded to an antenna structure with the proper impedance match so that the traveling wave directed toward the antenna leaves the device with none of the wave reflected. The other end is shorted between upper and lower strips, forming a totally reflective end that reflects the other traveling wave and sends it down the device right behind the first traveling wave. Thus, the static E-field with extent $10 L$ and amplitude $2 E_0$ is converted into a traveling electromagnetic wave of length $20 L$ and amplitude E_0 .

For 1 GHz operation with the fundamental of the square wave pulse, the wavelength, $\lambda = 2 L$, must be set to

$$L = \frac{\lambda}{2} = \frac{c}{2f},$$
$$\approx 15 \text{ cm}$$

for an air filled device.

Thus, the length of a plate determines the frequency of operation of the device. It can also be seen that the selection of 10 segments or elements with a reflecting end yields a pulse 10 cycles (at 1 GHz) in duration. Without the reflecting end, 20 elements would be needed.

e. Design Considerations

(1) Switching Requirements

It has been tacitly assumed in the previous discussion that the switches do not degrade the performance of the device. For this to be nearly true, the switches should meet the following criteria:

- (1) Switch closure, t_c , in 1/4 cycle or less (at 1 GHz, $t_c = 1/4$ ns).
- (2) Switch synchronization, t_s , 1/4 cycle or less (at 1 GHz, $t_s = 1/4$ ns).

These criteria are based on the fact that there is little spectral content in a waveform above a frequency given by $f = 1/t_r$, where t_r is the risetime which is equivalent to t_c , and on the fact that, viewing each element as an individual radiator, more than 1/4 cycle phase difference between elements results in excessive incoherence with a resulting reduction in power. Reference (2) provides a more extensive treatment of these criteria.

(2) Breakdown Limitations

There are two time periods during which the frozen E-field device might experience breakdown; while it is charging and after it is switched and the pulse is in the midst of exiting the device. Further, the charging period should be treated two ways in order to account for the two distinct ways in which energy can be introduced.

One way of charging the device is to slowly increase the potential of the plates. In this case, breakdown is limited to the static field limit, for example $\sim 30,000$ V/cm for dry air at one atmosphere. The other way of charging is to very rapidly (say in 1 ns) increase the potential to above the static field limit. If fast enough, the system can be overvolted (i.e., exceed the static breakdown field strength) without breakdown occurring before the device can be deliberately switched. In Appendix A this is discussed in some detail.

There are actually two field strengths that must be considered; the field within the gaps and the field between the two strips. The larger of the two will cause breakdown first and thus

determine the maximum allowed fields throughout the device. In the next section on energy storage, it will be shown that, for maximum energy storage, the field strength in these two regions should be equal. This will be assumed to be the case and no further distinction will be made.

During the exit of the pulse, midway along the last element on the reflective end, the device will be exposed to the full $2 E_0$ field strength for 5 ns, while at the antenna end, the field strength will be E_0 for 10 ns. If the device is not to experience breakdown, the most difficult of these conditions must be met, namely the field strength $2 E_0$, must not result in breakdown in 5 ns.

This is a more stringent requirement than the one for rapid charging in which the field strength achieved at the moment the device is switched may be so large that the breakdown lag time is less than 1 ns. As a result, the limiting consideration is that breakdown does not occur while the pulse exits the device. It will be assumed that the charging rate is at least fast enough to provide this field strength.

Two examples of what this breakdown limitation implies can be given. For air at 1 atmosphere the field strength with a 5 ns breakdown lag time is found from Reference (4) to be

$$E(\text{air}, 1 \text{ atm}) = 53,000 \text{ V/cm} = 5.3 \times 10^6 \text{ V/m.}$$

For SF_6 at 100 atmospheres, it is found to be

$$E(\text{SF}_6, 100 \text{ atms}) \cong 7,600,000 \text{ V/cm} = 7.6 \times 10^8 \text{ V/m.}$$

(3) Energy Storage Requirements

Consider a fixed potential $\pm V$ to be on each plate element given by

$$V = \frac{1}{2} E_g d$$

where E_g is the field between the gap and is assumed to be uniform (this can be accomplished using Rogowski configured gaps). The field between the plates, E_p , is then

$$E_p = V/D$$

and the stored energy of a single element, U , is then

$$\begin{aligned} U &= \frac{1}{2} \epsilon_0 E_p^2 AD \\ &= \frac{1}{2} \epsilon_0 (V/D)^2 AD \\ &= \frac{1}{2} \epsilon_0 V^2 A/D \end{aligned}$$

where A is the plate element area. Therefore, if d is fixed and E_g is set equal to the maximum field strength allowed from breakdown considerations, V is a constant and U is maximized by minimizing D . However, D must not get so small that $E_p > E_g$. As a result, D is $1/2 d$ for maximum U .

The design requirements of 10^{12} volts at 1 GHz for 10 cycles imply an energy content of the 1 GHz component of the square wave of 10^4 joules. A Fourier decomposition of a square wave reveals that the fundamental contains only one-half the total energy. Therefore, a

total energy U_T of 2×10^4 joules must be stored in the static field assuming that no losses occur because of such effects as finite switch resistance when the unfrozen pulse traverses the device. If the losses resulted in a triangular shaped output with the same peak amplitude as for the square wave, then the first harmonic would have only $4/\pi^2$ as much energy as in the first harmonic of the square wave. For there to be 10^4 joules at 1 GHz, 5×10^4 joules would have to be stored.

Using SF_6 at 100 atmospheres, the volume required to store this energy can be calculated. Note that $\epsilon \approx \epsilon_0$ and that the total length of the device will then be $10L = 1.5$ m. Then, considering all components making up the square wave and assuming no losses

$$\begin{aligned} \text{Volume} &= U_T / \frac{1}{2} \epsilon_0 E_p^2 \\ &= 7.82 \times 10^{-3} \text{ m}^3. \end{aligned}$$

This volume can be obtained using plates with $W = 105$ cm and $d = 1$ cm so that $D = 1/2$ cm. The value for d is around the upper limit on what might possibly be switched, within the switching requirements, using a UV laser, according to Bittis and Guenther (Reference(3)) provided an optical system were used to illuminate all of the gap at the same time.

f. Conclusions

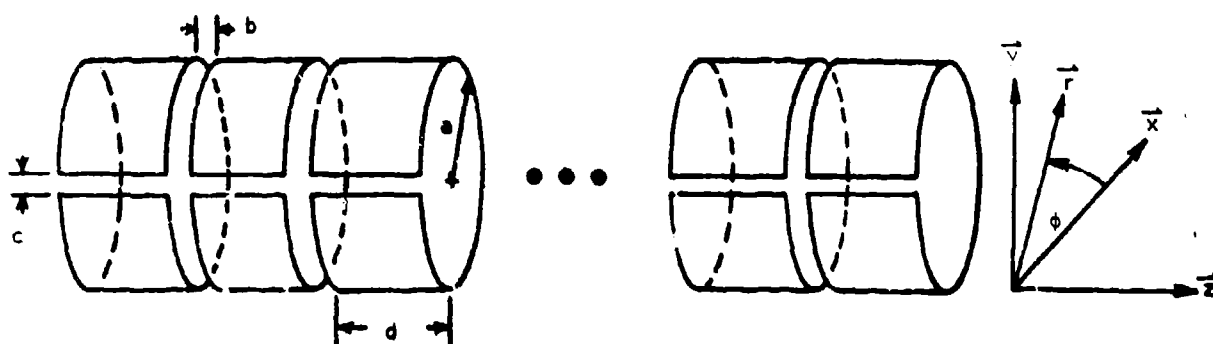
This device type appears promising, however, the need for high energy storage capabilities and fast, coherent switching are conflicting. Whether this conflict can be resolved while meeting design requirements will be examined in the In-Depth Analysis of Promising Devices, Section III.

2. FROZEN B-FIELD DEVICES

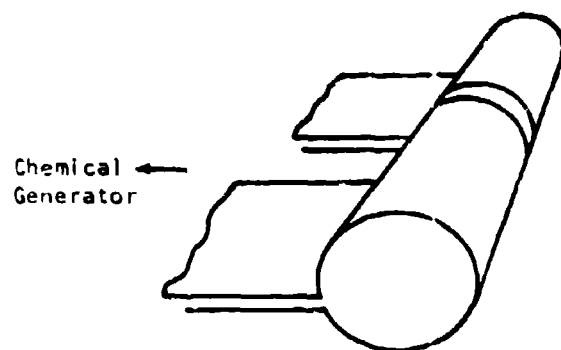
a. Slotted Frozen B-Field Device

(1) Configuration

The device under consideration has the following configuration.



It is composed of 10 individual cylinders or elements, each of which is separated from its neighbors by a gap of size b and each element has an axial slot of width c . An element is d long and a in inner radius with wall thickness e . A set of transmission lines connected to a common chemical generator feeds current to each cylinder of the apparatus. The transmission lines are connected to each slot as shown below.



The feed lines from the chemical generator to the transmission lines are alternately reversed to generate B-fields of opposite sense in the cylinders.

(2) Principle of Operation

The current from the chemical generator forces an azimuthal current I_ϕ around the cylinders. This current then produces an H_z within the cylinders which represents stored energy. The cylinders are separated by the gaps to insure azimuthal current flow.

For this stored energy to be radiated, current and charge distributions must be free to flow to support a propagating field. It is this freeing of charge and current distribution that represents the "unfreezing" of the stored energy which is determined by a static or near static distribution and, hence, referred to as a "frozen wave."

A more detailed analysis of these statements can be made by considering a TE_{11} mode propagating down a cylinder whose dimensions are such that the wave will propagate. The non-zero fields are

$$H_z = C_1 J_1 \left(\frac{y_{11} r}{a} \right) \cos \phi e^{i(\omega t - kz)}$$

$$H_r = -i (k C_1 / h) J_1' \left(\frac{y_{11} r}{a} \right) \cos \phi e^{i(\omega t - kz)}$$

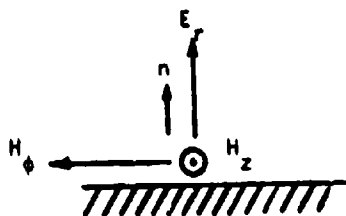
$$H_\phi = i (k C_1 / h^2) J_1 \left(\frac{y_{11} r}{a} \right) \frac{1}{r} \sin \phi e^{i(\omega t - kz)}$$

$$E_r = (\omega \mu / k) H_\phi$$

$$E_\phi = -(\omega \mu / k) H_r$$

where C_1 is a constant, J_1 is the first order Bessel function, y_{11} is the first root of J_1' , ω is the frequency, k is the wave number, a is the cylinder radius and $h = y_{11}/a$.

Looking down the axis near a small segment of the cylinder wall the fields appear as



since $E_\phi = H_r = 0$ at the surface.

There will be a surface current $J_{s\phi}$ flowing in the ϕ direction, and related to the magnetic field strength by the vector relation $\vec{J}_s = \vec{n} \times \vec{H}$, which in this case becomes $J_{s\phi} = -H_z$. A surface charge density appears on the surface, the value of which is given by $\rho_s = D_r = \epsilon E_r$. Since H_z and E_r , along with the other fields, propagate down the guide, so must the current and charge distribution.

The current distribution can propagate down the guide even if there are gaps such as in the slotted B-field device. This is because of displacement current across the gap to the next element. However, there must be a conducting bridge between elements for a physical charge to flow, hence, the slotted B-field device with gaps would not support a TE_{11} mode.

For a TE_{01} mode there are no tangential E-fields at the surface, as is true for all modes. Further, there is no radial E-field. Thus, no charge distributions are required by the TE_{01} mode and the slotted B-field device with gaps would support this mode.

To unfreeze the stored energy in this device then requires that the cylinder slots be closed removing the chemical generator from the circuit and thus removing the constraints on the current distribution.

With the current distribution unfrozen, the TE_{01} mode could propagate. If the gaps were also shorted, then the charge distribution would also be unfrozen and the other modes could propagate.

Unfreezing the current and/or charge distribution allows the frozen field to propagate. However, it does not determine how much of the field will propagate.

The amount that propagates is determined by the value of $\nabla_t H_z$, the transverse gradient of H_z . $\nabla_t H_z$ determines E_t and B_t which in turn determine how large a Poynting vector, S_z , there is down the guide. If

$$\nabla_t H_z = 0$$

then $E_t = B_t = S_z = 0$ and no energy propagates down the guide.

There are two ways to obtain $\nabla_t H_z \neq 0$. First consider the static case which takes account of the finite length of the cylinders. The H field for $I_\phi = \text{constant}$ will diverge as it leaves the cylinder and $\nabla_t H_z \neq 0$ over most of the cylinder. However, at the middle of the length of the cylinder, the field will still be uniform and $\nabla_t H_z = 0$ across the cylinder at this point. Consequently, B_t and $E_t = 0$ for this surface and no net energy flows.

Second consider the dynamic case. Let $I_\phi = Kt$, $K = \frac{dI}{dt} = 4 \times 10^{12}$ A/sec for 1 μsec as provided by a Sandia current generator using a dielectric fuse. Assuming a symmetric decay, this can be decomposed into sinusoidal current components.

The largest component will be

$$C_0 I_0 \cos \omega_s t$$

where $C_0 = \frac{4}{\pi^2}$ $\omega_s = \pi/1 \text{ usec} \rightarrow f_s = \frac{\omega_s}{2\pi} = \frac{1}{2} \times 10^6 \text{ Hz}$

$$I_0 = 4 \text{ MA.}$$

Since $f_s \ll 1 \text{ GHz}$, the wavelength will be large compared to the cylinder's dimensions. Thus a uniform current distribution is set up around the cylinder that varies as $\sin \omega t$. This results, ignoring fringing, in an internal field that goes as $J_0\left(\frac{\omega_s r}{c}\right)$.

(3) Modal Decomposition¹

Assuming that the current and/or charge distributions have unfrozen, it remains to decompose the field into the allowed modes. The field (the instant after unfreezing) that may now propagate has the same configuration as the static field just before unfreezing, provided losses are small during the switching. Taking this to be the case, the field can now be decomposed; first, axially into sinusoidally varying terms, then, transversely into the Bessel functions corresponding to the allowed modes.

The length of the cylinders imposes axial periodicity on the system. The field H_z , assumed uniform along z within each cylinder but alternating in sense, can be written as

$$H_z = H(r, \phi) \frac{4}{\pi} \sum \frac{1}{N} \sin \frac{N\pi z}{d} \\ N = 1, 3, 5, \dots$$

¹ The modal decomposition performed here and in subsequent sections makes use of sinusoidally varying functions in the axial decomposition that are of finite extent. That is, the sinusoidal functions are set to zero outside the device or beyond the extent of the pulse ejected from the device, depending on the case being treated. This is the same type of decomposition performed on a vibrating string of finite length fixed at the endpoints. See Appendix D for a detailed discussion.

The allowed sinusoidal waves have

$$k_z = \frac{N\pi}{d}, N = 1, 3, 5, \dots$$

The transverse field $H(r, \phi)$ can next be decomposed.

Since $E_z = 0$, only TE modes need be considered. The boundary conditions require that $J'_n(y_{nm}) = 0$ at the cylinder's surface. The radial field dependence must be expressed in terms of a modified Fourier-Bessel series. The azimuthal dependence need not be considered since there is no ϕ variation in the field.

An arbitrary function $f(r)$ can be expanded on the interval $0 \leq r \leq a$ in a modified Fourier-Bessel series as

$$f(r) = \sum_{m=1}^{\infty} A_m J_n(y_{nm} r/a),$$

where y_{nm} is the m^{th} root of $\left. \frac{dJ_n(r)}{dr} \right|_{r=a} = 0$ and the coefficients

A_m are given by,

$$A_m = \frac{2}{a^2 \left(1 - \frac{n^2}{y_{nm}^2}\right) J_n^2(y_{nm})} \int_0^a f(r) r J_n(y_{nm} r/a) dr.$$

Since $H(r, \phi) = H(r)$ (i.e., does not depend on ϕ) it can be expanded as

$$H(r) = \sum_{m=1}^{\infty} H_m J_0(y_{0m} r/a)$$

where

$$H_m = \frac{2}{a^2 J_0(y_{0m})^2} \int_0^a H(r) r J_0(y_{0m} r/a) dr.$$

Note that if $H(r)$ is assumed constant with value C or equivalently $\nabla_t H_z = \nabla_r H(r) = 0$, then the expansion becomes the trivial one that

$$H(r) = C J_0\left(\frac{y_{00} r}{a}\right) = C J_0(0) = C.$$

Setting

$$H(r) = \frac{C_0 I_0}{d} J_0(\omega_s r/c)$$

$$H_m = \frac{2 C_0 I_0/d}{a^2 J_0(y_{0m})^2} \int_0^a J_0\left(\frac{\omega_s r}{c}\right) J_0\left(\frac{y_{0m} r}{a}\right) r dr.$$

The largest H_m will be H_1 for those modes that propagate.

$$H_1 = \frac{2 C_0 I_0/d}{a^2 J_0(y_{01})^2} \int_0^a J_0\left(\frac{\omega_s r}{c}\right) J_0\left(\frac{y_{01} r}{a}\right) r dr$$

$$\approx \kappa \int_0^a \left\{ r - \frac{1}{4} \left[\left(\frac{\omega_s}{c} \right)^2 + \left(\frac{3.83}{a} \right)^2 \right] r^3 \right.$$

$$\left. + \left[\frac{1}{64} \left(\frac{3.83}{a} \right)^4 + \frac{1}{16} \left(\frac{\omega_s}{c} \right)^2 \left(\frac{3.83}{a} \right)^2 \right] r^5 \right.$$

$$\left. - \frac{1}{256} \left(\frac{\omega_s}{c} \right)^2 \left(\frac{3.83}{a} \right)^4 r^7 \right\} dr$$

where $\kappa = 2 C_0 I_0/d a^2 (.403)^2$,

$$\begin{aligned}
&= \kappa \left\{ \frac{a^2}{2} - \frac{a^4}{4} \left[\left(\frac{\omega_s}{c} \right)^2 + \left(\frac{3.83}{a} \right)^2 \right] + \frac{a^6}{6} \left[\frac{1}{84} \left(\frac{3.83}{a} \right)^4 + \frac{1}{16} \left(\frac{\omega_s}{c} \right)^2 \left(\frac{3.83}{a} \right)^2 \right] \right. \\
&\quad \left. - \frac{a^8}{8} \frac{1}{256} \left(\frac{\omega_s}{c} \right)^2 \left(\frac{3.83}{a} \right)^4 \right\} \\
&= \kappa \left\{ \left[\frac{a}{2} \left(\frac{3.83}{a} \right) - \frac{a^3}{16} \left(\frac{3.83}{a} \right)^3 + \frac{a^5}{6} \frac{1}{54} \left(\frac{3.83}{a} \right)^5 \right] \frac{a}{(3.83)} \right. \\
&\quad \left. - \frac{a^4}{16} \left(\frac{\omega_s}{c} \right)^2 + \frac{a^6}{96} \left(\frac{\omega_s}{c} \right)^2 \left(\frac{3.83}{a} \right)^2 - \frac{a^8}{8 \cdot 256} \left(\frac{\omega_s}{c} \right)^2 \left(\frac{3.83}{a} \right)^4 \right\} \\
&\approx \kappa \left\{ J_1(3.83) \frac{a^2}{3.83} - \frac{a^4}{16} \left(\frac{\omega_s}{c} \right)^2 \left[1 - \frac{a^2}{6} \left(\frac{3.83}{a} \right)^2 + \frac{a^4}{8 \cdot 16} \left(\frac{3.83}{a} \right)^4 \right] \right\} \\
&= -\kappa \frac{a^4}{16} \left(\frac{\omega_s}{c} \right)^2 \left[1 - \frac{3.83^2}{6} + \frac{3.83^4}{128} \right] \\
&= \kappa \frac{a^4}{16} \left(\frac{\omega_s}{c} \right)^2 (.23) \\
&= - \left(\frac{\omega_s a}{c} \right)^2 \epsilon_0 \frac{I_0}{d} \times .177 \\
&= \left(\frac{\omega_s a}{c} \right)^2 \frac{4}{\pi} (.177) H_0,
\end{aligned}$$

where $H_0 = I_0/d$.

Note that the larger a is, the better the efficiency of the TE_{01} mode.

(4) Geometry for 1 GHz Operation of TE₀₁ Mode

κ and ω are related by

$$k_z = \frac{N\pi}{d} = \left[\omega^2 \mu \epsilon - \left(\frac{y_{nm}}{a} \right)^2 \right]^{1/2}$$

Solving for d

$$d = \frac{N}{2 [f^2 - f_c^2]^{1/2} \sqrt{\mu \epsilon}}$$

where

$$f = \frac{\omega}{2\pi}$$

$$f_c = \frac{\omega_c}{2\pi}, \quad \omega_c = \frac{1}{\sqrt{\mu \epsilon}} \left(\frac{y_{nm}}{a} \right)$$

(c denotes cutoff frequency)

For the TE₀₁ mode, require $f = 1$ GHz and $f_c < 1$ GHz. Further, if d is not to be excessive, f_c must be appreciably smaller than f . To make f_c smaller, since y_{01} is fixed, a is required to be larger. Larger a is desirable since it makes H_1 larger. It also increases the volume in which energy can be stored.

Let $f = \sqrt{2} f_c = 1$ GHz so that $f_c = .707$ GHz and let the cylinder be air filled so that $1/\sqrt{\mu \epsilon} = c$. Considering only the sin $\pi z/d$ component axially with $N = 1$, then

$$d = \frac{c}{2 f_c} = \frac{3 \times 10^{10} \text{ cm/sec}}{2 \cdot 707 \times 10^9 / \text{sec}} = 21.2 \text{ cm}$$

and

$$a = \frac{1}{2\pi \sqrt{\mu\epsilon}} \frac{y_{01}}{f_c} = \frac{c}{2\pi} \frac{3.83}{.707 \times 10^9} = 25.9 \text{ cm}.$$

This represents an acceptable geometry that will result in a TE_{01} mode propagating above cutoff at a frequency of 1 GHz.

(5) Radiation Efficiency

The magnitude of the field in the TE_{01} mode, represented by H_1 can now be evaluated.

$$H_1 = \left(\frac{\pi \times 10^6 \times 25.9}{3 \times 10^{10}} \right)^2 \left(\frac{4}{\pi^2} \right) (.177) H_0$$

$$= .53 \times 10^{-6} H_0$$

The ratio, R, of energy radiated by the TE_{01} mode to the total energy stored goes as

$$R = \frac{\int [H_1 J_0(y_{01} r/a) \sin \frac{\pi z}{d}]^2 dv}{\int H_0^2 dv}$$

$$= \frac{\int_0^d \int_0^{2\pi} \int_0^a \left[H_1 J_0 \left(\frac{3.83 r}{a} \right) \sin \frac{\pi z}{d} \right]^2 r dr d\phi dz}{H_0^2 \pi a^2 d}$$

$$= \frac{(.53 \times 10^{-6})^2 H_0^2 \times \frac{1}{2} d \times 2\pi \times \int_0^a J_0^2 \left(\frac{3.83 r}{a} \right) r dz}{H_0^2 \pi a^2 d}$$

$$= \frac{(.53 \times 10^{-6})^2}{2} J_o^2 (3.83)$$

$$2 \times 10^{-14}$$

This represents an extremely low efficiency.

(6) Conclusions

For higher modes namely TE_{on} , $n = 2, 3, 4 \dots$ the relation between k and ω can be solved using the values of a and d selected for the TE_{01} mode. As can be seen, the frequency of propagation will be higher and the coefficients even lower.

If the peaking time for the current were 10^2 faster, then the ratio of energy radiated to energy stored would be 10^8 times higher or 4×10^{-6} . In order to radiate the required 10^4 joules, a total energy of 2.5×10^9 joules would have to be stored. At present, only 10^6 to at most 10^7 joules are available from an explosive current generator and switch times only 10^1 times faster than the 1 μ sec time used are considered state-of-the-art or beyond.

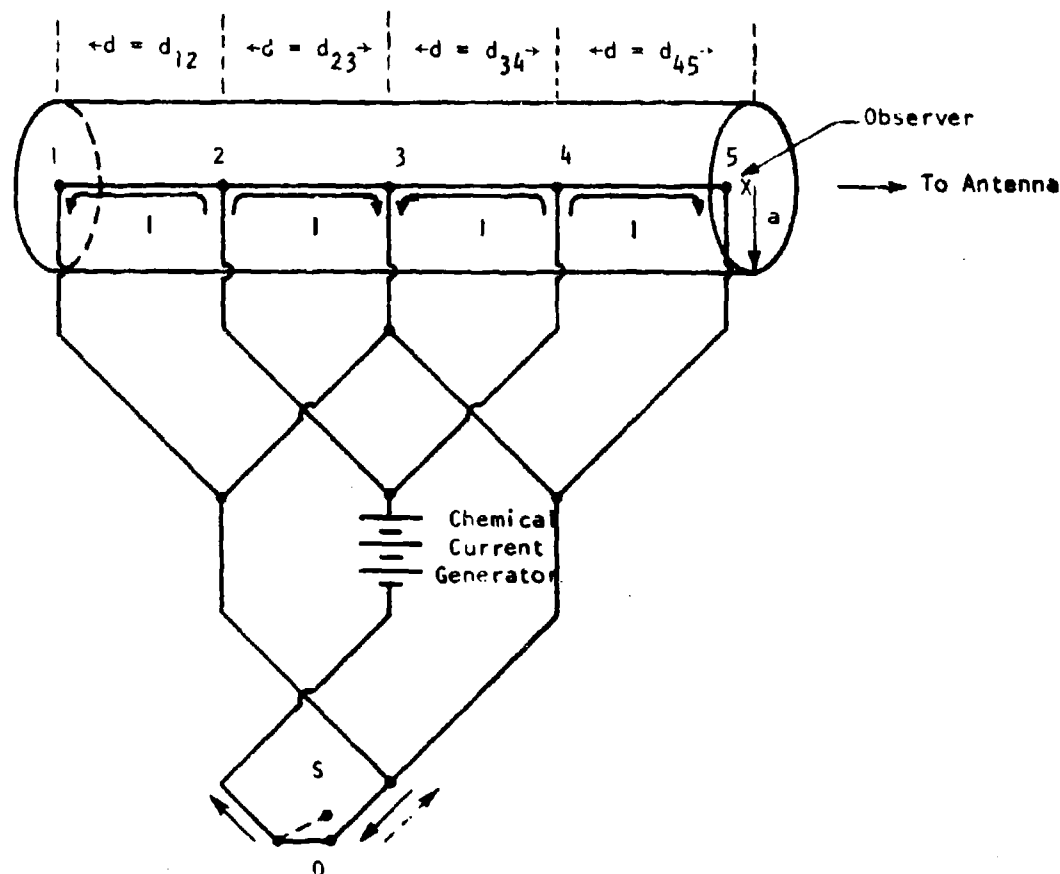
The explanation for these gross inefficiencies lies in the fact that $H(r) \approx \text{constant}$, so that $CJ_o (Y_{00} r/a) = C \cdot 1$ is the leading term in the expansion. Had the device been made superconducting, this term just represents the static field resulting from the current that persists unchanged around the elements. If the device were not superconducting, the current would be dissipated in joule heating, resulting in the collapse of the associated field.

b. Coaxial Frozen B-Field Device

(1) Using Remote Switch

(a) Configuration

The device under consideration has the following configuration when used with a remote switch.

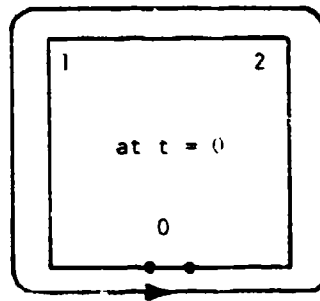


It is shown here with four current elements instead of the 10 needed for meeting the design requirements when one end is reflective and the other coupled to an antenna structure. This was for illustrative purposes only. This design provides alternating current elements along the center conductor of a coaxial transmission line. The currents are produced by a remote chemical current generator such as the Sandia type. They are fed to the central conductor by transmission lines that are alternately reversed to provide the current reversal. Each current element, namely 1 to 2, 2 to 3, etc., are equidistant along the transmission lines from a fast opening switch S at point 0 (i.e., to say d_{01} , the distance from the switch to point 1, equals d_{02} and so forth).

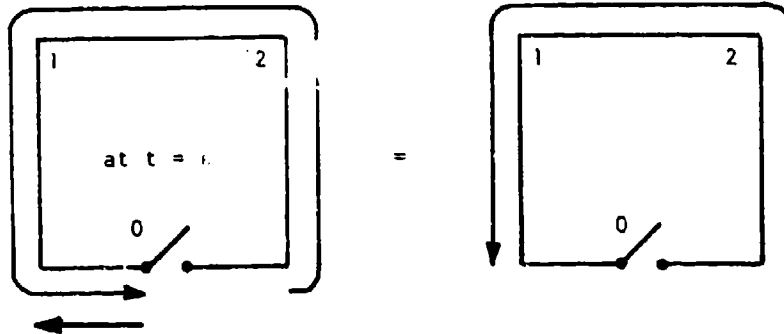
(b) Principle of Operation

When S is opened at $t = 0$, current on the right of the open is reflected back up the line, while the current already past the open, on the left, continues to the left; the reflected current cancels the original current. The time behavior for the 012 loop is shown below assuming no current losses on the lines:

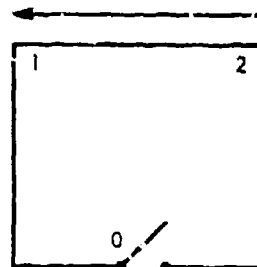
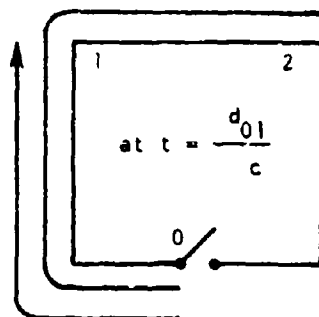
Current Distribution with Switch Closed



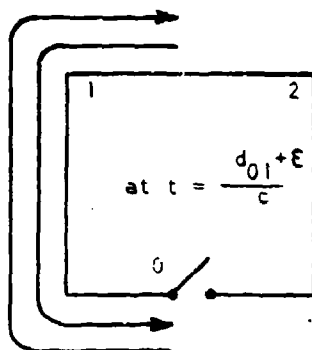
Shortly After Switch is Opened



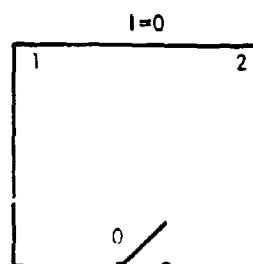
Current Distribution on Coaxial Portion of the Loop Only at $t = \frac{d_{01}}{c}$



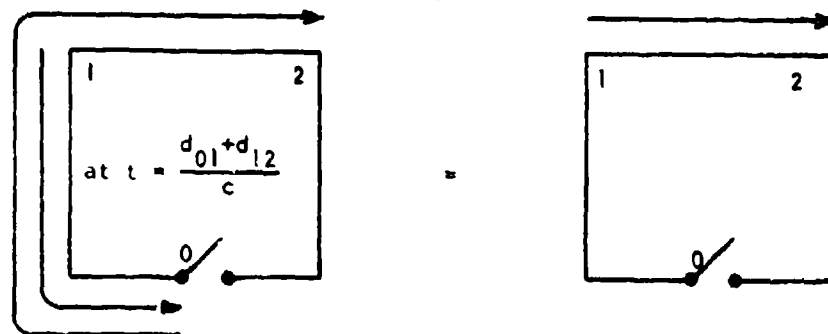
Complete Cancellation, Current Distribution Zero



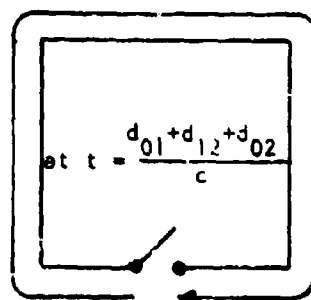
=



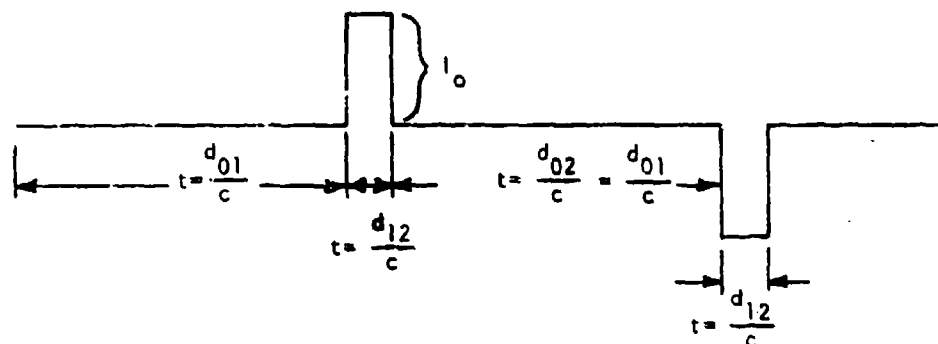
Current Reversal on Coaxial Portion of Loop



Current Reversal on Entire Loop



This behavior along the central conductor is represented by a square wave distribution of current that at time $t = d_{01}/c$ splits into two traveling waves going in opposite directions along the central conductor. They travel over a segment or equivalently propagate in time for $t = d_{12}/c$, then stop for a time $t = d_{02}/c = d_{01}/c$ and then the pattern repeats itself. An observer placed just beyond the end of the device on the side that feeds an attached antenna will see a current that varies in time as



(c) Modal Decomposition

This current distribution in time may be represented by

$$I(t) = \sum_n I_n(t) = \frac{2d_{12}}{D} I_0 \sum_{n=1}^{\infty} \sin \frac{n\pi}{2} \frac{\sin(\frac{1}{2} n\pi d_{12}/D)}{\frac{1}{2} n\pi d_{12}/D} \sin \frac{n\pi t}{D/c}$$

where

$$D = d_{01} + d_{12}.$$

Geometry considerations show that for S equidistant from the end points of the coaxial current elements (10 in all for the actual device)

$$d_{01} = \sqrt{2} \cdot 10 \cdot d_{12}$$

thus,

$$d_{01} \gg d_{12}$$

so that

$$d_{01} \approx D.$$

If the nth term provides the 1 GHz output, then

$$\omega_n = n\pi c/D = 2\pi \times 10^9$$

or

$$D = \frac{rc}{2 \times 10^9} = n \times 15 \text{ cm.}$$

(d) Efficiency

1 Efficiency, $d_{12} = 15$ cm

Let $d_{12} = 15$ cm, then

$$d_{01} \approx 2\sqrt{10} d_{12} \approx 14.2 \times 15 \text{ cm}$$

which implies

$$n = 15.$$

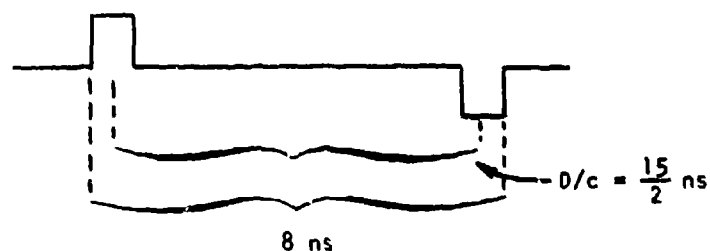
The energy content of the 15th harmonic, U_{15} , compared to the total energy, U_T , is given by

$$\begin{aligned} \frac{U_{15}}{U_T} &= \frac{\int_0^{D/c} I_{15}^2(f) dt}{\int_0^{D/c} I^2(f) dt} \\ &= \frac{\frac{4 d_{12}^2 I_0^2}{D^2} \left(\sin \frac{15\pi}{2} \right)^2 \left(\frac{\sin 1/2\pi}{1/2\pi} \right)^2 \int_0^{D/c} \sin^2 \left(\frac{15\pi t}{D/c} \right) dt}{\left(d_{12}/c \right) I_0^2} \end{aligned}$$

$$= \frac{8 d_{12}}{D\pi^2}$$

$$= 5.35 \times 10^{-2}.$$

During a 10 ns period one cycle is completed, i.e.,



Hence, only 1/10 of the power is transmitted in this time. The overall efficiency is then 5.35×10^{-3} .

2 Efficiency, $d_{12} = 1 \text{ cm}$

If, instead of this configuration, $D = 15 \text{ cm}$, then $n = 1$ gives 1 GHz and $d_{12} \approx 1 \text{ cm}$. The energy content of the first harmonic, U_1 , compared to U_T , is given by

$$\begin{aligned} \frac{U_1}{U_T} &= \frac{\int_0^{D/c} I_1(t)^2 dt}{\int_0^{D/c} I(t)^2 dt} \\ &= \frac{\left(4 d_{12}^2 I_0^2 / D^2\right) \left(\sin \pi/2\right)^2 \left(\frac{\sin \frac{\pi}{30}}{\pi/30}\right)^2 (1/2 D/c)}{\left(d_{12}/c\right) I_0^2} \\ &\approx \frac{2 d_{12}}{D} = \frac{2}{15} . \end{aligned}$$

Since the whole pulse will exit in 10 ns, this is also the overall efficiency. However, the device is now only 10 $d_{12} = 15$ cm long.

3 1 GHz Output Comparison

The efficiency storage volume product, assuming equal radii of inner and outer conductors and equal field strengths, is just a measure of the energy radiated at 1 GHz by the two configurations. Comparison of the $d_{12} = 1$ cm and $d_{12} = 15$ configuration yields products of

$$\frac{2}{15} (0.15 \text{ m}) \text{ versus } (5.35 \times 10^{-3}) 1.5 \text{ m}$$

or

$$2 \times 10^{-2} \text{ versus } 0.8 \times 10^{-2}.$$

There is little difference in the energy radiated by either device at 1 GHz.

(e) Breakdown Limitations

1 $d_{12} = 1$ cm Device

Because of the relatively long duration between half square waves, which allows an avalanche to "quench," it will be assumed that breakdown must be caused by a single half square wave of duration 3.3×10^{-2} ns. Hence, the breakdown lag time for the gas filling the device must be 33 ps or greater. This determines the maximum allowed E-field after switching. From Reference (4)

$$E(\text{air}, 1 \text{ atm}, 33 \text{ ps}) = 3.0 \times 10^7 \text{ V/m}$$

$$E(\text{SF}_6, 100 \text{ atm}, 33 \text{ ps}) = 1 \times 10^9 \text{ V/m.}$$

The value using SF_6 at 100 atms in the $d_{12} = 1 \text{ cm}$ device is only slightly greater than that for the frozen E-field device using SF_6 at 100 atms. Thus, the energy density is only slightly greater. Since the device requires a smaller volume than the frozen E-field device and has an efficiency of 2/15, its energy output at 1 GHz is approximately 1/50 the frozen E-field device output.

$$\underline{2} \quad \underline{d_{12} = 15 \text{ cm Device}}$$

For this case, the breakdown lag time must be equal to or greater than the duration of a single half square wave, namely 0.5 ns. From Reference (4)

$$E(\text{air}, 1 \text{ atm}, 0.5 \text{ ns}) = 9.5 \times 10^6 \text{ V/m,}$$

$$E(\text{SF}_6, 100 \text{ atm}, 0.5 \text{ ns}) = 7.6 \times 10^8 \text{ V/m.}$$

The value using SF_6 at 100 atms in the $d_{12} = 15 \text{ cm}$ device is the same as for the frozen E-field device using SF_6 at 100 atms. While this device is not reduced in size, its efficiency is only .005 and, hence, it too is inferior to the frozen E-field device in energy storage capabilities.

(f) Conclusion

The use of a single remote switch obviates any switch synchronization problems. However, as a trade-off it has significantly lower efficiency or energy storage capabilities than the frozen E-field devices.

(2) Using Multiple Switches

(a) Configuration

A fast opening switch at all the end points of the axial current elements would avoid the efficiency loss noted in the previous subsection. These switches would have to meet the following requirements:

- (1) Simultaneity in switching is 250 ps or better.
- (2) Switch time duration is 250 ps or less.
- (3) The switches result in only a minor perturbation to the device electrically.

It should be noted that these conditions appear to be virtually impossible to meet now or in the near future. (See Reference (5)) Nonetheless, this configuration, in theory, provides the most efficient operation. It also provides the simplest configuration of this device for formal analysis which follows.

(b) Principle of Operation

Assume that the device has switches at the ends of each current element and that they meet the three requirements given above and are loss free. Then the time behavior of the current on the central conductor is that of two traveling square waves after the switches are thrown. This is just the previous result for the remote switch with $d_{01} = d_{02} = 0$.

(c) Modal Decomposition

The static field at $t = 0$ given by the two traveling waves superimposed, one on top of the other, must be formally decomposed into the allowed modes of the system. First it can be decomposed in the axial direction. The square wave current $I(z)$ can be decomposed as

$$I(z) = I_0 \frac{4}{\pi} \sum_{n=1,3,5,\dots} \frac{1}{n} \sin \frac{n\pi z}{d_{12}}.$$

The current $I(z)$ results in a field

$$H(z) = \frac{I(z)}{2\pi r}.$$

This field can also be decomposed axially as

$$H(z) = H_0 \frac{4}{\pi} \sum_{n=1,3,5,\dots} \frac{1}{n} \sin \frac{n\pi z}{d_{12}},$$

where $H_0 = \frac{I_0}{2\pi r}.$

Writing this in terms of traveling sine waves, $H(z)$ becomes

$$H(z) = H_0 \frac{2}{\pi} \sum_{n=1,3,5} \frac{1}{n} \left[\sin \frac{(n\pi z - \omega t)}{d_{12}} + \sin \frac{(n\pi z + \omega t)}{d_{12}} \right].$$

The axial components of $H(z)$ should now be expanded in terms of the allowed modes of the coaxial system. This expansion is trivial since each axial component decomposes exactly into a TEM wave. This follows from the fact that the H-field of a TEM mode is given by

$$H = \frac{I}{2\pi r}.$$

The E-fields of the two traveling waves with the same value of k have equal and opposite values, and at the moment the static field is freed, the E-fields of the two waves cancel. This holds for each pair of traveling sine waves and explains why there is no E-field present in the static field.

(d) Efficiency

The relation between ω and k for each traveling sine wave pair is

$$\omega = ck = c \frac{n\pi}{d_{12}} .$$

For $d_{12} = 15$ cm, one must have $n = 1$ for the TEM mode that propagates out of the device at a frequency of 1 GHz. The ratio of the energy in this mode to the total stored is given by

$$\frac{\int_0^{d_{12}} \sin^2 \frac{\pi z}{d_{12}} dz}{\int_0^{d_{12}} 1^2 dz} = \frac{1}{2} .$$

Half of the stored energy is propagated out of the device at the frequency of interest and the efficiency is extremely high. The problem is to develop an opening switch that meets the requirements.

(e) Design Considerations

1 Multiple Switch Simultaneity Considerations

An example of switching difficulties is illustrated by considering explosively driven mechanical switches. Assume the feed lines and the axial lines resting on the feed lines are finely machined to a 10^{-3} cm tolerance. Further assume that an explosively driven plate impacts the axial line imparting a velocity on the order of .3 - .5 cm/ μ sec. The variation in switching times is the combined tolerance divided by velocity, namely

$$t = \frac{2d}{V}$$

$$= \frac{2 \times 10^{-3} \text{ cm}}{.5 \text{ cm}/\mu\text{sec}}$$

$$= 4 \text{ nanoseconds.}$$

Thus, the simultaneity in switching times using mechanically obtainable velocities is more than a factor of ten too long for machined tolerance of 10^{-3} cm.

Electrically activated switches capable of high power loads are state-of-the-art or beyond at 100 ns for their switching time (5).

2 Breakdown Limitations

Three distinct periods exist during which the B-field device might arc. They are:

- (1) The charging period where the nonzero rate of current change, $di/dt \neq 0$, results in a voltage given by $L di/dt$.
- (2) A quasistatic period where the current is roughly constant, $di/dt = 0$, and the B-field is at a maximum.
- (3) The period after the switches are thrown and the stored energy is released and propagates through the device as an electromagnetic wave.

To within an order of magnitude, the voltage encountered for a single element during the charging period is given approximately by taking the maximum current to be $\sim 10^6$ amperes, the risetime to be ~ 1 usec, so that $di/dt \cong 10^{12}$ amps/sec, and the inductance to be $\cong 100$ nanohenries¹. Then

$$di/dt \cong 10^5 \text{ volts}$$

For element length $L = 15$ cm, the electric field strength is $< 10^6$ V/m. Thus, it can be seen, using representative values for the coaxial frozen B-field device and a risetime obtainable with the best peaking circuits currently used, that this voltage is below the breakdown strength of air and well below the breakdown strength of gases such as SF_6 . Hence, arcing is not a problem during this period.

The maximum B-field encountered in the next period can be as high as several megagauss. Electrical breakdown is not associated with even such large B fields. However, structural integrity could be a problem because of the magnetic pressures generated by the field, which at several megagauss, can destroy a steel cylinder. The device must maintain its structural integrity for a time period of only a few microseconds. Using thick walls for the cylinder, 1-2 centimeters, would insure that the cylinder, while deforming, would remain unbroken for this time period (6).

After switching, the static B-field (amplitude $2 B_0$) is transformed into two traveling waves just as in the frozen E-field device, only in this case at the reflective end a field of amplitude $2 B_0$ persists for 5 ns, while at the antenna end a field of amplitude B_0 persists for 10 ns. Since the E-fields are in quadrature to the B-fields,

¹The approximate output and required inductive load of the Sandia type generator with a peaking circuit was used to establish these values.

an E-field amplitude of $2 E_0$ persists for 5 ns at the reflective end of the device. Thus, the same breakdown limitations exist for the coaxial frozen B-field device with multiple switches as do for the frozen E-field device.

3 Energy Storage Requirements

If the field within the coaxial B-field device were uniform, then the storage volume required would be the same as for the frozen E-field device. This follows because only as much energy as can be transmitted without breakdown should be stored. Any additional stored energy will result in breakdown and seriously degrade performance. Since the coaxial device does not have a uniform field, a somewhat larger volume would be required. The ratio is given by

$$R = \frac{\int_0^{2\pi} \int_a^b \left(\frac{a}{r}\right)^2 r d\theta dr}{\pi(b-a)^2} = \frac{2a^2}{(b-a)^2} \ln(b/a)$$

where b is the outer conductor radius and a the inner conductor radius.
For $b = 2a$

$$R = 2 \ln 2 = 1.39.$$

Hence, the frozen coaxial B-field device with multiple switches has slightly less storage capability than the frozen E-field device.

c. Frozen B-Field Devices: General Switching Considerations

A frozen B-field device relies on constant current distributions that are switched to free the current and unfreeze the frozen B-field. Two different kinds of switches can be employed, those that close and those that open. Three geometries that can be used are:

- (1) A linear array of cylinders with a small gap between each one with the cylinders axially slotted. This is the slotted frozen B-field device which acts as a waveguide with respect to propagating energy.
- (2) A linear array of cylinders with a small gap between them. The cylinders support an axial current along them. This device acts as a waveguide.
- (3) A linear array of cylinders with coaxial loops that carry the currents. This is the coaxial device. It acts as a transmission line.

For (1), the current flows azimuthally around the cylinders alternating direction between cylinders. The force between current elements of adjacent cylinders is repulsive and the current distribution takes on a minimum energy configuration where all the forces are balanced. Geometries (2) and (3) have the currents running in line and no force is generated.

Assume all the different configurations are made superconducting so that ohmic losses need not be considered. The result of having no forces or balanced forces between current elements is that current is strictly conserved (i.e.,

$$\nabla \cdot \vec{J} = 0$$

both before and after closing a switch). This implies that from the equation of continuity for charge and current

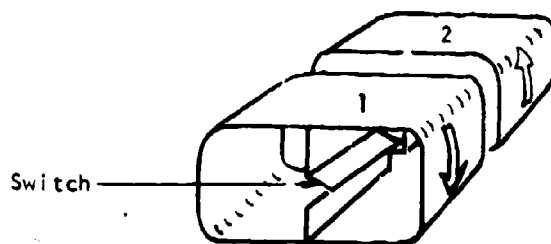
$$\frac{\partial \rho}{\partial t} = 0.$$

Thus, with $\vec{D} = 0$ initially (before switching), have $\vec{D} = 0$ after switching. This follows from Maxwell's equation

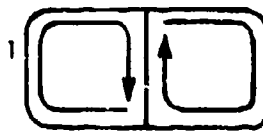
$$\nabla \cdot \vec{D} = 4\pi\rho.$$

When no D-field is generated (and in this case no E-field), the system cannot radiate.

As an example consider the following system:

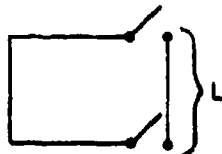


There are two current carrying superconducting loops with current flowing in opposite directions. The rightmost side represents the generator and the leftmost side the slotted B-field device while the switch represents the slot that is closed when the device is switched. The current distribution has reached equilibrium when the switches are closed forming two loops in place of each original loop. The current will now flow around the two loops as



Note that $\nabla \cdot \vec{J} = 0$ and in fact $\vec{J} = \text{constant}$ and that this is unchanged by switching.

On the other hand, consider any of the geometries in the superconducting state using opening switches. The result can be shown diagrammatically in a simplified fashion using a single current loop.



When the switches are open, the current oscillates along the segment L as described in the treatment of the coaxial device. In this arrangement, $\nabla \cdot \vec{J} \neq 0$ so that $\partial \rho / \partial t \neq 0$ and a D-field is generated and radiation results.

Had resistance been considered for closing switches, the ohmic losses would have resulted in the characteristic exponential decay of the B-field. This would have resulted in a D-field decaying in the same manner. Forming $\vec{E} \times \vec{H}$ one finds that no power is radiated.

The conclusion is that only opening switches can lead to radiation for any of the frozen B-field device configurations that employ a constant current distribution that is switched.

3. FERROELECTRIC DEVICE

a. Introduction

Barium titanate, BaTiO_3 , a well known ferroelectric, has the needed energy storage capabilities, a physical transition mechanism that takes the material from the polarized to the unpolarized state, thereby releasing the stored energy, and a sufficiently short switching time of the ferroelectric domains. There is still the problem of achieving switching simultaniety and the problem of efficiently coupling the device to an antenna.

b. Energy Storage Capabilities

At room temperature the spontaneous polarization, P_s , from Reference (7) is

$$P_s = .78 \times 10^5 \text{ esu}$$

and the dielectric constant ϵ from Reference (8) is

$$\epsilon \approx 2000 \epsilon_0.$$

The stored energy/volume, U/V , in gaussian units, is given by

$$U/V = \frac{1}{8\pi} \left(\frac{D^2}{\epsilon} + \mu H^2 \right)$$

where

$$D = \epsilon E = E + 4\pi P$$

$$= 4\pi P, \quad \text{when } E = 0.$$

Thus

$$U/V \cong 2 \text{ joules/cm}^3.$$

This implies for 10^4 joules of stored energy

$$V = .5 \times 10^4 \text{ cm}^3.$$

c. Transition

BaTiO_3 undergoes a state change from ferroelectric \rightarrow paraelectric (no spontaneous polarization) at a transition temperature $T_t = 390^\circ \text{ K}$. As a function of pressure (Reference (9)) the change in transition temperature is given by

$$dT_t/dp = -4.0^\circ \text{ to } -6.7^\circ \text{ K/kbar.}$$

To reduce T_t to room temperature, $\sim 300^\circ \text{ K}$, and thereby induce the ferroelectric \rightarrow paraelectric transition, requires an overpressure Δp of no more than

$$\begin{aligned}\Delta p &= \Delta T / |dT/dp| \\ &= 90^\circ \text{ K} / \frac{4^\circ \text{ K}}{\text{kbar}} \\ &= 22.5 \text{ kbar}\end{aligned}$$

Thus, explosives which are capable of producing pressures on the order of 100 kbar are more than capable of depolarizing BaTiO_3 .

d. Switching Times (References (7) and (8))

Using a field of $E = 100 \text{ kV/cm}$ and a sample 0.1 mm thick, a switching time of 10 nsec has been obtained. This time, t_s , is defined as the time necessary for the current output from a ferroelectric that is depolarized by a current pulse to drop by 95 percent of its maximum value. For high field strengths, such as 100 kV/cm

$$t_s = kE^{-n},$$

where $n \approx 1.5$.

Thus, a field of 465 kV/cm yields a $t_s = 1 \text{ ns}$ for a sample 0.1 mm thick.

This field can be related to an equivalent pressure using

$$P = Zd + EX,$$

where

- P = polarization
- Z = stress
- d = piezoelectric strain constant
- E = electric field
- X = dielectric susceptibility.

By setting

$$Zd = EX$$

the stress that changes P by an amount equal to the change from $E = 465 \text{ kV/cm}$ can be found. For BaTiO_3 ,

$$d \approx 10^{-5} \text{ cm/statvolt},$$

$$X = (\epsilon - 1)/4\pi \approx 2000/4\pi,$$

and

$$E = 465 \text{ kV/cm} = 1.55 \text{ kstatvolt/cm}.$$

Hence

$$\begin{aligned} Z &= \frac{EX}{d} = \frac{1.55 \times 10^3 \text{ statvolt/cm} \cdot 2 \times 10^3 / 4\pi}{10^{-5} \text{ cm/statvolt}} \\ &= 2 \times 10^{10} \frac{\text{dynes}}{\text{cm}^2} = 20 \text{ kbar}. \end{aligned}$$

From this result, it is concluded that switching times of $\sim 1 \text{ ns}$ are possible with chemical explosives using thin films of $\sim 1 \text{ mm}$ thickness.

This time, however, is not the total switching time. It must include the time required for the depolarizing shock front to transverse the material. Assuming explosive films on either side of a thin plate of BaTiO_3 , time t_p required to shock the whole BaTiO_3 plate is

$$t_p = \frac{\frac{1}{2} D}{V_s}$$

where

D = thickness

V_s = shock velocity.

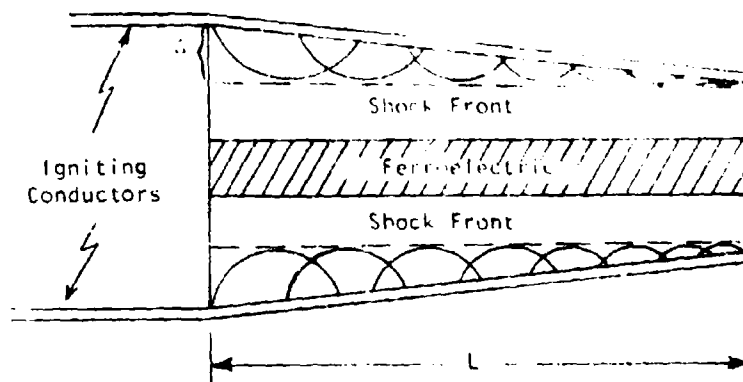
Taking V_s to be approximately 3×10^5 cm/sec and requiring t_p to be 1 ns

$$\begin{aligned} D &= 2 t_p V_s \\ &= 6 \times 10^{-4} \text{ cm.} \end{aligned}$$

A film of this thickness will be traversed by the depolarizing shock in 1 ns or less depending on shock velocity. Since the overpressure will result in the individual domains of the BaTiO_3 depolarizing in less than 1 ns, the total time to depolarize a film of this thickness is on the order of 1 ns.

e. Simultaneity

The means by which simultaneity in firing the ferroelectric device may be achieved is based on a suggestion by W. Quinn. The explosive surrounding a single film of ferroelectric would be tapered so that the path length difference from the igniting conductor to the ferroelectric would exactly compensate for the time it takes the current to flow across the conductor. This can be illustrated as follows:



The amount of taper given by Δ is selected so that

$$\frac{\Delta}{c_s} = \frac{L}{c},$$

c_s is the shock velocity and c is the conduction current velocity which is just the velocity of light in the media.

For

$$L = 25 \text{ cm}, c_s = 0.3 \text{ cm/usec and } c = 3 \times 10^{10} \text{ cm/sec},$$

then

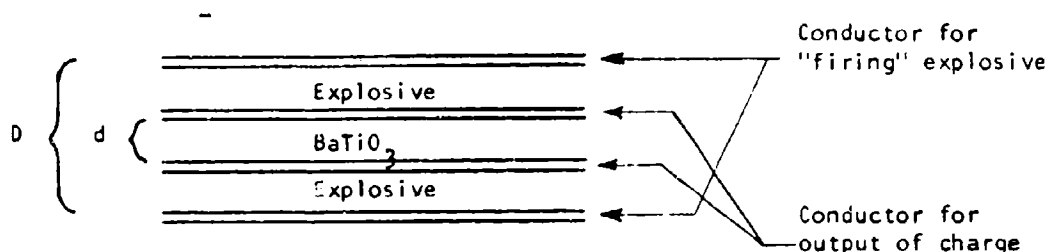
$$\Delta = 2.5 \times 10^{-4} \text{ cm.}$$

(The choice of $L = 25 \text{ cm}$ is shown in the next section to correspond to the dimensions of a cube containing the required amount of ferroelectric material and explosives.)

f. Coupling of the Ferroelectric Device to an Antenna

(1) Capacitive Analysis

The ferroelectric device requires a volume of at least $0.5 \times 10^4 \text{ cm}^3$ of BaTiO_3 and the thickness of the BaTiO_3 must be no greater than $6 \times 10^{-4} \text{ cm}$. A "sandwich" type arrangement satisfies this requirement. Typically, it would have the following structure



The thickness D of the complete sandwich would be approximately three times d , the thickness of a BaTiO_3 layer. Hence the total storage volume would be $1.5 \times 10^4 \text{ cm}^3$. This could be obtained from a cube with side $L \approx 25 \text{ cm}$. Assuming that $d = 6 \times 10^{-4} \text{ cm}$, this cube would represent a stack of n capacitors where

$$n = \frac{L}{d} = \frac{0.25 \text{ m}}{1.8 \times 10^{-5} \text{ m}} \approx 1.5 \times 10^4$$

and the capacitance of a single layer would be

$$C = \frac{A\epsilon}{d} = \frac{(0.25 \text{ m})^2 \cdot 2 \times 10^3 \epsilon_0}{6 \times 10^{-6}} \approx 1.85 \times 10^{-4} \text{ farads.}$$

If the individual layers were connected in parallel to feed an antenna via a transmission line, the total capacitance C_{total} would be

$$C_{\text{total}} = nC$$

$$\approx 2.9 \text{ farads.}$$

The time behavior of a current discharging from a capacitor into a resistive load (equal to the impedance of the transmission line which must be matched to the antenna impedance) is

$$i_0 e^{-t/RC}$$

For the current to fall to e^{-1} in 10^{-9} sec with a $C = 2.8$ farads, R would be given by

$$R \approx 4 \times 10^{-10} \text{ ohms.}$$

This is clearly not feasible.

Even if each layer were to drive an individual antenna the resistance would have to be

$$R \approx 5 \times 10^{-6} \text{ ohms.}$$

This is still too low to be practicable.

(2) Transmission Line Analysis

The ferroelectric system treated as a capacitive problem was shown to have an unacceptable decay time. W. Quinn proposed that it be configured so that it could be treated as a transmission line.

Assuming this to be the case and that the system is appropriately impedance matched to an antenna so that no losses result at this juncture, the losses within the line can be calculated.

At 1 GHz, Fatuzzo and Merz⁽⁸⁾ show that the loss tangent, $\tan \delta$, for BaTiO_3 is approximately $\frac{1}{6}$ for a temperature $T = 160^\circ\text{C}$ which is well above the Curie point. It will be assumed that an equivalent point can be reached using explosives; a reasonable assumption based on the prior results where an overpressure obtained with explosives dropped the Curie point to room temperature or below. Then the loss tangent would again be $\sim \frac{1}{6}$. This implies that

$$\epsilon'' = \frac{\epsilon'}{6}$$

where ϵ' is the real part of the dielectric constant and ϵ'' the imaginary part.

Since k is defined as

$$k = \sqrt{\mu \epsilon} \omega,$$

the wave number can be written as

$$\begin{aligned} k &= \sqrt{\epsilon' + i\epsilon''} \sqrt{\mu} \omega \\ &= \sqrt{1 + i/6} \sqrt{\epsilon' \mu} \omega \\ &\approx (1 + i/12) k_0, \end{aligned}$$

where

$$k_0 = \sqrt{\epsilon' \mu} \omega.$$

The wave train behaves as

$$e^{ikx} = e^{ik_0 x} e^{-k_0 x/12}$$

For

$$x = 10 \lambda = \frac{20 \pi}{k_0},$$

the negative exponent is evaluated to be

$$e^{-k_0 x/12} = e^{-\frac{20\pi/12}{12}}$$

$$= \frac{1}{188}.$$

Thus, the trailing edge of the wave train is down in amplitude by a factor of ~200 from that of the leading edge. Examining the behavior of the loss tangent shows that little can be gained by going to higher temperatures or equivalent pressures (8).

4. MOVING MIRROR APPROACHES

a. Introduction

Generally speaking, a moving mirror approach toward a high frequency, high energy output device can be treated in one of two ways. First, it can be viewed as a doppler shifting device. Second, it can be treated as the moving boundary of a cavity. In each case the moving mirror frequency shifts the EM waves and transfers energy to them. The energy transfer comes about from the work done by the moving mirror against the radiation pressure of the EM wave.

The feasibility of the moving mirror concept to act as a frequency transformer will now be examined. The highest output frequency from a chemical generator that employs some kind of peaking circuit is no more than 1 MHz. This will be the input to a moving mirror system that must supply an output at 1 GHz. A frequency upshift of 1000 is then required.

b. Single Reflection

The simplest approach is "to bounce" the 1 MHz signal off a moving mirror once. The doppler shifted frequency is given by

$$\omega' = \frac{\omega}{\sqrt{1-v^2/c^2}} \left(1 - \frac{v}{c}\right)$$

for an incident beam normal to the reflecting surface.

For $\omega' = 1000 \omega$

$$v \approx .999999c.$$

This velocity is unobtainable using chemical explosives. It is possible to achieve this velocity with a plasma that is electrically accelerated. However, the apparatus would be very large, on the order of a large particle accelerator since the velocity required implies an energy of 256 MeV for each electron in the plasma.

Additional problems are imposed by the electron density required for the plasma to be reflective. The incident electromagnetic radiation frequency must be less than the characteristic plasma frequency for the radiation to be reflected by the plasma. The plasma frequency is given by ⁽¹⁰⁾

$$\omega_p = \left[\frac{4\pi n_o q^2}{m \epsilon_o} \right]^{1/2}$$

where

n_o is the electron density

q is the electron charge

m is the electron mass

ϵ_o is the dielectric constant of space.

Taking $\omega = \omega_p = 2\pi \times 10^9$ then

$$n_o \approx 10^{10} \text{ electrons/cm}^3.$$

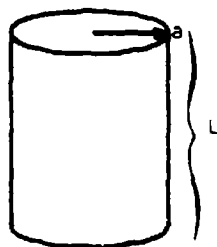
This density is far in excess of what even large accelerators are designed to handle.

c. Multiple Reflections

The above considerations demonstrate that multiple reflections must be used. In order to use this approach a cavity must be employed, otherwise the multiple reflections would invariably lead to excessive losses. The reflected beam would escape from between the two boundaries needed for multiple reflections unless the boundaries were perfectly flat and the incident waves were exactly normal to the boundary.

The cavity would require a switchable inlet and outlet port to admit radiation at 1 MHz and output it at 1 GHz. It will be assumed that perfectly switchable ports are available. The problems associated with the cavity are twofold. First is losses. Second is size. The size problem is, in fact, an insurmountable one. For the cavity to absorb energy at 1 MHz that will subsequently be frequency upshifted by the moving boundary, it must be "cut" to resonate at 1 MHz. For a cylindrical cavity, this implies for the lowest possible mode of excitation, the length L is ≈ 200 meters and the radius $a > 88$ meters. This has been derived as follows:

For a cylindrical cavity, as shown



the lowest TM mode, TM_{010} , has a frequency

$$\omega_{010} = 2.405 \frac{c}{a}$$

or

$$a = 115 \text{ m @ 1 MHz.}$$

For the lowest TE mode, TE_{111} , the resonance frequency is

$$\omega_{111} = 1.841 \frac{c}{a} \left(1 + 2.912 \frac{a^2}{L^2} \right)^{1/2}.$$

If $L = 2.03 a$ then $\omega_{111} = \omega_{010}$ and

$$a \approx 100 \text{ m, } L \approx 200 \text{ m @ 1 MHz.}$$

As $L \rightarrow \infty$

$$\omega_{111} = 1.841 \frac{c}{a}$$

and

$$a = 88 \text{ meters.}$$

Setting this problem of size aside there are still other problems connected with the use of such cylinders.

(1) Chemically Compressed Cylinder

The velocity associated with a chemical explosion is no better than $\sim .3 - .5 \text{ cm}/\mu\text{sec}$. The time to compress the cylinder axially would be $\sim 40-70 \text{ msec}$. Alternately, the cylinder could be compressed radially. The time required would be $\geq 18 \text{ msec}$.

The attenuation occurring within these times can be roughly calculated. Assume that the cavity is excited with the TM_{010} mode. The Q for this mode, with the cavity uncompressed, so that $\omega \approx 2\pi \times 10^6$, is (11)

$$Q = \frac{1}{2\pi} \left(\frac{\mu}{\mu_c} \right) \left(\frac{1}{1 + \frac{L}{a}} \right) \frac{L}{\delta} \approx 10^5$$

if $L \approx a$.

The energy behaves in time (ignoring the frequency shift) as

$$U(t) = U_0 e^{-f_0 t/Q}.$$

For a time of 20 msec, corresponding to the compression time,

$$U(20 \text{ ms}) = U_0 e^{-.2}.$$

Initially then, based on the Q for the uncompressed cavity, the loss is small. However, the loss during the last stages of compression must also be examined.

For the compressed cavity

$$Q \approx 3 \times 10^3$$

since $L = 1000a$ and $\delta \propto \omega^{-1/2}$.

Then for a characteristic time during which this configuration holds, taken to be 1 ms, and with $\omega \approx 2\pi \times 10^9$

$$U(1 \text{ ms}) \approx U_0 e^{-3 \times 10^3}.$$

This represents an excessive loss.

(2) Plasma "Tuned" Cylinder

Another way of moving a boundary of the cavity is with a moving, reflective plasma. This method will not work with a plasma acting as a moving "plug" traveling down the axis of the cylinder. The reason is quite simple. The plasma will be quenched wherever it comes in contact with the cylinder wall.

What will work is to confine the plasma to a small region of the cylinder using an externally applied axial B-field to compress a plasma produced in the tube prior to energy being admitted. Once the cavity is fully excited, the axial B-field is collapsed allowing the plasma to expand and retune the cylinder. This method avoids quenching by the walls but suffers from other problems. One problem is that the cavity would have to be approximately as large as before. Another problem is that radial compressions of only a factor of 30 or so are achievable with the plasma densities needed to keep the plasma reflective at the frequencies contemplated ⁽¹²⁾.

Finally, the energy used to compress the plasma must be significantly greater than the energy represented by the admitted EM wave.

Otherwise expansion will be restricted by the pressure of the EM wave. This implies that far more energy must be expended on compression than on generating the 1 MHz EM wave which already represents a large amount of energy.

5. PLASMA OSCILLATIONS ⁽¹⁰⁾

Another approach using plasmas is to excite the plasma into oscillation with an incident EM field. The plasma could then be compressed by an externally applied B-field in a fashion similar to that discussed in the previous section. The magnetic field at large x compared to the plasma size is given by

$$B = \left[\frac{e \kappa^2 \phi_0^2 \sqrt{\pi} L^3}{32 \sqrt{2} m c \omega_c} \right] (\vec{\gamma} \cdot \vec{n}) (\vec{\gamma} \cdot \vec{x}) \frac{\sin(2 \omega_c t - \kappa x)}{x} e^{-3 \omega_c^2 L^2 / 8 c^2}$$

where

$2 \omega_c$ = frequency of emission

$\kappa = \sqrt{3} \omega_c / c$

$\phi_0 = \int_0^{\infty} (1 + \gamma \cdot \vec{x}) e^{-x^2/L^2} = \text{source size}$

$L^2 = KT/4 n n_0 e^2$ is the Debye length

ω_c = Plasma frequency

n_0 = Electron density

γ = Gives a measure of the deviation from spherical symmetry in the oscillation.

Since ω_c goes as $n_0^{1/2}$ the compression increases n_0 and hence increases the frequency of emission, $2 \omega_c$. During compression the plasma will lose energy through

radiation. Only if compression is sufficiently fast will sufficient energy remain for the desired output.

Another problem is the size. In order for the system to radiate appreciably, it must have

$$\omega_c L \sim c$$

so

$$L = \frac{c}{\omega_c} = \frac{3 \times 10^{10} \text{ cm/sec}}{2\pi \times \frac{1}{2} \times 10^9}$$

$$= 10 \text{ cm at } 1 \text{ GHz}$$

Since ω_c is proportional to $n_0^{1/2}$, the density n_0' at 1 MHz required for appreciable radiation is

$$n_0' = n_0 / 10^6$$

where n_0 is taken to be the density at 1 GHz for appreciable radiation.

Since L is proportional to $n_0^{-1/2}$

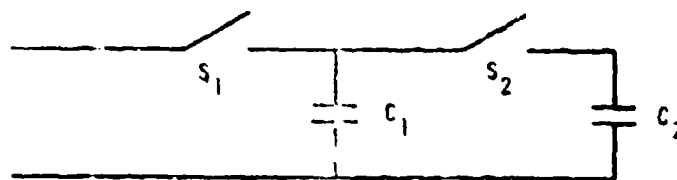
$$L' = 10^3 L = 100 \text{ m}$$

where L' is the length at 1 MHz for appreciable radiation and L is the length at 1 GHz for appreciable radiation. Again the size is excessive.

A caveat is appropriate. The equation for the radiation field is derived assuming that the fractional energy loss of a radiating electron is negligible over the time of interest. Further, the treatment used to derive the B field assumes small perturbations.

6. CAPACITIVE DISCHARGE APPROACH

The system considered has the configuration illustrated below



The first capacitor C_1 is charged while S_1 is closed and S_2 is open. Upon completion of charging, S_1 opens and next S_2 closes. This results in charge flowing to the second capacitor C_2 whose capacitance equals C_1 .

It seems clear that a state will be reached in which charge will be equally distributed on both capacitors. This will result in a net loss in capacitively stored energy. The energy capacitively stored by C_1 before S_2 closed was

$$U = \frac{1}{2} Q_0^2 / C.$$

After S_2 closes

$$U = \frac{1}{2} (Q_0 / 2)^2 / C_1 + \frac{1}{2} (Q_0 / 2)^2 / C_2 = \frac{1}{4} Q_0^2 / C_1.$$

If this state were one of equilibrium and there were no ohmic losses, radiation would account for the energy loss. However, it will now be shown that this is not an equilibrium system and that the system does not radiate.

The system must obey Kirchoff's voltage law and, in order to satisfy this condition, the self inductance of the wire connecting the two capacitors must be included. Then the differential equation describing the circuit's behavior is

$$\frac{Q}{C} + \frac{C}{L} \frac{dI}{dt} - \frac{(Q - Q_0)}{C} = 0$$

where $C = C_1 = C_2$.

Then

$$(2Q - Q_0) + \frac{C}{L} \frac{dI}{dt} = 0$$

subject to the initial conditions that at $t = 0$

$$Q = Q_0 \text{ and } I = 0.$$

The differential equation can be written as

$$2I + \frac{C}{L} \frac{d^2 I}{dt^2} = 0$$

with the solution

$$I = I_0 \sin \omega t$$

where $\omega = (2/LC)^{1/2}$.

At $t = 0$ the differential equation yields

$$\frac{Q_0}{C} + \omega I_0 = 0.$$

Thus

$$I_0 = \frac{-Q_0}{\omega C}.$$

At $t = t_0$, $Q = Q_0/2$ so that $dI/dt = 0$ which implies $I = I_0$. The magnetic field associated with this current is $B = I_0$ and the energy associated with this field is

$$U = \frac{1}{2} L I_0^2 = \frac{1}{4} Q_0^2 / C.$$

This accounts for all the energy and, as a result, radiation does not occur.

This analysis holds with complete rigor provided the circuit is small compared to a wavelength. If, however, the loop were on the order of a wavelength, then a radiation resistance would have to be added. The system would then act like a circular loop antenna and radiate weakly.

By the principle of complementarity, a similar system consisting of inductors rather than capacitors will have the initial stored energy distributed inductively and capacitively after switching and all of the energy will be accounted for in this fashion so that radiation does not occur.

7. SYNCHROTRON RADIATION

Electrons are injected into a solenoid perpendicular to an axial magnetic field within the solenoid. The electrons are required to have an orbital radius less than the radius of the solenoid and an angular frequency $\omega = 2\pi \times 10^9$ so that what radiation results will be at 1 GHz. Assume that the magnetic field can attain a strength of 10^2 webers/m² ($= 1$ MC), then

$$\gamma = \frac{1}{\sqrt{1 - \frac{v^2}{c^2}}} = \frac{qB}{m_0 \omega} \left(1 - \frac{v^2}{c^2} \right)^{1/2}$$

and from this, noting that $\left(\frac{m_0 \omega}{qB} \right) \approx 0$,

$$r = \frac{c}{\omega} \left[1 - \left(\frac{m_o \omega}{qB} \right)^2 \right]^{1/2}$$

$$= .047m.$$

Further

$$v = \frac{qBr}{m} = \frac{qBr}{m_o} \left(1 - \frac{v^2}{c^2} \right)^{1/2}$$

so that

$$v = \frac{\left(\frac{qBr}{m_o} \right)}{\left[1 + \left(\frac{qBr}{m_o c} \right)^2 \right]^{1/2}} = \frac{c}{\left[1 + \frac{1}{\left(\frac{qBr}{m_o c} \right)^2} \right]^{1/2}}$$

$$\approx \frac{c}{1 + \frac{1}{2 \left(\frac{qBr}{m_o c} \right)^2}} \approx c \left[1 - \frac{1}{2 \left(\frac{qBr}{m_o c} \right)^2} \right]$$

$$= c \left[1 - \frac{1}{1.53 \times 10^7} \right].$$

This is an extremely high velocity. To see just how high, consider the energy the electron must acquire to reach this velocity.

$$E = \frac{mc^2}{\left(1 - \frac{v^2}{c^2}\right)^{1/2}} = \frac{.511 \text{ MeV}}{\left(1 - \left[1 - \frac{1}{1.53 \times 10^7}\right]^2\right)^{1/2}}$$

$$= 1.42 \text{ BeV.}$$

This velocity is obtainable only with large particle acceleration making this approach impractical.

It should be noted that a more sophisticated approach has been tried at Cornell University and at the Naval Research Laboratory. A rippled magnetic field is used into which an intense, mildly relativistic electron beam is injected. V. L. Granastein, et. al. ⁽¹³⁾ have reported obtaining 25 MW of coherent synchrotron radiation from a 500 keV, 15 kA, 50 ns electron beam with an approximately 10 percent magnetic field ripple ($\Delta B/B_0$).

Dr. Granastein indicated, in a private conversation, that the microwave energy is primarily obtained from the kinetic energy of the beam. The rippled field configuration results in high frequency cyclotron oscillations that convert the energy of motion into microwave radiation at ~ 8 GHz. It appears that a stronger B field as obtainable from chemical generators would serve only to increase the frequency of operation and not to significantly increase the output. This point is not yet well established and it is possible that higher outputs might be obtained with the multimegagauss fields obtainable by chemical means.

8. BRILLOUIN AND RAMAN SCATTERING ^(14, 15)

Both Brillouin and Raman scattering result from an EM wave being scattered by an interaction with a vibrational mode of a material medium. The scattered wave is frequency shifted by an amount corresponding to that of

the vibrational mode from which the scattering takes place. Raman scattering involves the optical modes of the system while Brillouin scattering involves the acoustic modes. ~~Either approach corresponds to a variation~~ on the moving mirror theme.

Raman scattering is not practical as the energy of the incident EM wave must correspond to frequencies in the visible or near infrared to be able to interact with the optical modes.

Brillouin scattering is impractical since the acoustic velocity of modes that can in practice be excited in a material are so low. While higher velocity modes exist and, if excited, could interact with the incident EM wave, the interaction would be extremely weak unless these modes are strongly excited. The strong excitation of these high frequency modes cannot be achieved in practice.

9. CANDIDATE RANKINGS

The devices studied can be divided into three categories:

(1) Those that don't work or are highly impractical:

- (a) Slotted B, in general any B-field device using closing switches.
- (b) Moving mirrors.
- (c) Raman and Brillouin Scattering.
- (d) Synchrotron Radiation.
- (e) Capacitive Discharge Approach.

(2) Those that are barely workable with major design requirement changes:

- | | | |
|----------------------------------|---|--|
| (a) Compressed Cavity | } | All of these approaches failed because of size. If size is reduced by 100 fold then device would be ~1 meter in extent. Faster compression times and much lower losses would result. |
| (b) Cavity with Expanding Plasma | | |
| (c) Plasma Oscillations | | |

(3) Those that might be workable with or without minor design requirement changes:

- (a) Frozen E.
- (b) Ferroelectric Device.
- (c) Axial B, in general any B device using opening switches.

This last group represents the devices selected for in-depth study.

SECTION IV

MODIFIED DESIGN REQUIREMENTS

1. BREAKDOWN CONSIDERATIONS

a. General Discussion

In the generation of a spark, there is a formative period during which an initial electron, accelerated by the applied field, produces an electron avalanche that grows exponentially to 10^8 electrons, reaching a critical size. This period is referred to as the formative time, t_f . After this time, streamers are rapidly formed in a time period $1/10$ or less of the formative time⁽¹⁶⁾. In gaps, where the final current growth is limited by the external impedance, the streamer will represent typically 10^{12} to 10^{14} electrons. A more detailed treatment of these features is given in Appendix B, titled SPARK GAP TIME BEHAVIOR AND ITS MODELING.

This behavior is for "static" fields; however, it will be valid for the square wave varying field considered here if the period of the field does not approach the transit time t_o of electrons between collisions with gas molecules. Considering only thermal motion at room temperature and one atmosphere pressure, t_o is given by⁽¹⁷⁾

$$t_o = \left(\frac{2m}{\pi kT} \right)^{1/2} \lambda$$

where

k = Boltzmann constant

m = Mass of electron

T = Room temperature = 300°K

λ = Mean free path of the electron $\approx 3 \cdot 10^{-7} \text{ m.}$

Evaluating t_0 , it is found that

$$t_0 = 3.6 \times 10^{-12} \text{ sec}$$

Hence, our use of the "static field" behavior is valid for the frequencies of interest.

b. Inside the Frozen E- and B-Devices

In the analysis of the possible devices in Section III, it was assumed that breakdown must be avoided at any point that the pulse transversed. A free electron accelerated by the pulse's field could generate an avalanche of critical size in the formative period, but then the pulse must have left the region so that streamers would not be formed. This criterion can be stated as: the formative time, t_f , should not be less than the pulse duration, $t_{p,d}$. This insures that streamers will not form.

The formation of streamers within a device such as the frozen E-field device, would quickly short it out. With streamer velocities as high as $c/10$ and plate separations of ~ 1 cm, the time it would take would be $\sim 1/3$ ns. The criterion was applied near the reflecting end of the device where the field strength was a maximum for 5 ns to obtain a maximum allowed field strength. Using a pulse with this field strength, a streamer would be just ready to form as the pulse left this region so that a short would not be formed. However, as can be seen from the breakdown formative time curves for SF_6 at 100 atmospheres⁽⁴⁾, a negligible increase (<10 percent) in the field strength can halve the formative time. In which case, the short would be established before the pulse left the region at the reflecting end of the device and approximately the last half of the pulse would be seriously degraded. Had the device been air filled at 1 atmosphere, the electric field need only be increased ~ 20 percent to halve the formative time. Thus, the criterion that the pulse duration be equal to the formative

time, yields a field strength that is quite close to the actual maximum allowable field strength. It is a physically valid criterion inside the device for the conditions of interest.

c. Outside Any Device

Outside a device, the same criterion can be derived using a different argument. If the pulse duration is 1.1 times as long as the formative time, then streamers will be well formed. The antenna emitting the field will be large, on the order of a meter across. It will be assumed that the electric field is uniform across a cross sectional area of this size. Then the streamers established within this region will grow across dimensions of a meter before leaving the field and quenching. Hence, the number of electrons within a streamer should be at least equal or greater than those found with relatively small gaps (~1 cm), namely 10^{12} to 10^{14} electrons. It will be assumed then that each streamer has developed to 10^{14} electrons in the time equal to $1.1 t_f$. While this is only an approximation, note that if the time were increased to $1.2 t_f$, recalling that the streamer started at t_f and has grown twice as long at $1.2 t_f$ as at $1.1 t_f$, the number of electrons quoted can be easily exceeded since the growth rate of a streamer is so fast.

At an altitude of 20 kilometers, there are approximately 2-3 electrons/cm³(18). As a pulse with $t_{p.d.} = 1.1 t_f$ sweeps through a 1 cm³ volume at 20 km, there will be 2-3 streamers established with 2×10^{14} to 3×10^{14} electrons. Nitrogen predominates over oxygen in the atmosphere and is more readily ionized. The first ionization potential is 7.61 eV = 1.22×10^{-18} joules. Hence, the amount of energy u , required to generate these streamers in 1 cm³ is no less than

$$u = (2 \times 10^{14} \text{ electrons/cm}^3) (1.22 \times 10^{-18} \text{ joules/electron})$$

$$= 2.44 \times 10^{-4} \text{ joules/cm}^3.$$

From Figure 2 of Reference(4), the electric field strength, E , with $t_f = 9$ ns (since $t_{p.d.} = 10$ ns $\approx 1.1 t_f$) at 1/10 atmosphere (pressure at 20 km) is

$$E = 9,000 \text{ volts/cm} = 9 \times 10^5 \text{ V/m}.$$

The total energy flux, EF , of a pulse with this field strength across a 1 cm^2 area is

$$\begin{aligned} EF &= \left[\frac{1}{2} \epsilon_0 E^2 + \frac{1}{2} \mu_0 H^2 \right] ct \\ &= \epsilon_0 E^2 ct \\ &= 2.15 \times 10^{-3} \text{ joules/cm}^2. \end{aligned}$$

Ignoring the reduction in field strength due to loss, in less than 10 cm of travel, this energy will have been totally dissipated in generating streamers. Taking account of the losses, it can be seen that the field strength will be reduced to about the field given by the criterion that $t_{p.d.} = t_f$ so that streamers are not formed and little energy is lost to ionization processes.

At lower altitudes, such as 5 km, Figure 3.2-1 of Reference(18) can be extrapolated to give $\sim 1/2$ electron/cm³. The energy required to generate streamers in 1 cm^3 is then no less than

$$u = 0.61 \times 10^{-4} \text{ joules/cm}^3.$$

The air pressure at this altitude is $\sim 1/2$ atmosphere and the field strength with $t_f = 9$ ns at this pressure is

$$E = 27,400 \text{ V/cm} = 2.74 \times 10^6 \text{ V/m}.$$

The total energy flux, EF, of a pulse with this field strength across a 1 cm^2 area is

$$\begin{aligned} EF &= \epsilon_0 E^2 ct \\ &= 1.99 \times 10^{-2} \text{ joules/cm}^2. \end{aligned}$$

Then the path length, PL, over which this energy is dissipated, ignoring loss, is

$$\begin{aligned} PL &= \frac{EF}{u} \\ &= 3.26 \times 10^2 \text{ cm.} \end{aligned}$$

Even at this lower altitude, then, the field strength will be reduced to nearly that given by the criterion $t_{p.d.} = t_f$.

This result will break down at altitudes very close to sea level since the number of free electrons becomes very small. Hence, the criterion that the field strength not exceed that given by $t_{p.d.} = t_f$ will be assumed for altitudes of 5 km or greater. The 5 km figure itself is dependent on the accuracy of the extrapolation and should be considered only a rough guide. Below this altitude, Reference (19) should be consulted in order to determine the attenuation of the pulse.

2. ANTENNA SIZE AND POWER CAPABILITIES

Taking a 1 m^2 antenna aperture to be the largest allowable, the amount of power radiated from this size aperture can be found at an altitude of 5 km. Since the maximum field that can be transmitted over appreciable distances is that which obeys the criterion $t_{p.d.} = t_f$, the field strength is

$$E = 2.66 \times 10^6 \text{ V/m.}$$

The total energy transmitted is then

$$U = 187 \text{ joules}$$

so that the power, P, is

$$\begin{aligned} P &= U/t_{p.d.} \\ &= 1.87 \times 10^{10} \text{ watts.} \end{aligned}$$

For a square wave pulse, half of this power, 0.94×10^{10} watts, is at 1 GHz. At higher altitudes, the field strength drops, so that even less power is transmitted.

3. MODIFIED DESIGN REQUIREMENTS

For altitudes greater than ~5 km, the amount of power that can be effectively radiated from a 1 m^2 aperture at 1 GHz is approximately 1/100 or less than the design requirements call for. Since the device(s) should be expected to be able to operate over a wide altitude range, a reduced power requirement of 10^{10} watts at 1 GHz maximum will be used.

The reduction in energy content implied by the reduced power, it should be noted, can be offset somewhat by using more elements in a device so that a longer wave train is generated. While the wave train will have a larger $t_{p.d.}$ so that t_f is larger and the maximum E-field allowed is lower, the reduction in field strength is more than offset by the increased pulse duration. However, this cannot be carried too far or else synchronization problems set in.

Increasing the frequency of operation will not increase the power that can be transmitted from a fixed size aperture over the frequency range of interest. There is a point that can be found on Figure 2 of Reference (4) where a decrease in t_f and hence $t_{p.d.}$ is just offset by an increase in E^2 . This point has been found to be at $Pt_f = .38 \times 10^{-7}$ mm Hg sec. At one-half atmosphere this corresponds to $t_f = 10^{-10}$ seconds which implies that for a 10 cycle wave train, the frequency is 100 GHz. Above this point, the aperture can be made smaller and still transmit the same amount of energy in a 10 cycle wave train. Below this frequency, the aperture must get larger.

SECTION V

IN-DEPTH ANALYSIS

1. FROZEN E-FIELD DEVICE

a. Assumptions

In addition to the assumption of a 1 m diameter aperture with 1 GHz and 10 cycle operation, the following assumptions will be made:

- (1) Laser triggered switching using very high power UV laser will yield the required subnanosecond switching times and jitter needed for useful output.
- (2) Uniform fields between gaps obtained with Rogowski gap configuration.
- (3) Device overvolted to field strength that will yield propagating pulse with amplitude equal to that set by the breakdown avoidance limitation.
- (4) SF_6 between gaps at 100 atmospheres.
- (5) $d = 2D = 1$ cm for nearly uniform field throughout device.

b. Admissibility of a 1 cm Gap

The limit to how large the device can be made in terms of D is set by how large a d can be switched within the required times. A gap of 1 cm according to an AFWL paper ⁽³⁾ has been switched with as little as 0.1 ns jitter and a delay time of 4.5 ns.

While the closure time (time from bridged gap to complete voltage collapse) is not guaranteed to be below 0.25 ns and the gas used was Ar-N at ~ 4 atms instead of the SF₆ at 100 atms contemplated, this gap separation appears to be about the upper limit in spacing that may be feasible when a high power UV laser is employed to fire an overvolted gap. Further discussion of this question is presented in Appendix C.

c. Internal Electric Field Strength

For a 5 ns breakdown lag time, the E/p value can be found from Figure 2 of Reference (4) to be

$$E/p \geq 10^2.$$

Since p is assumed to be 7.6×10^4 mm Hg

$$E = 7.6 \times 10^6 \text{ V/cm} = 7.6 \times 10^8 \text{ V/m.}$$

d. Device Size as Required by Switch Closure Times

As seen in Appendix B, SPARK GAP TIME BEHAVIOR AND ITS MODELING, the final time behavior of the spark gap switch is governed by its inductance. The breakdown lag time represents a period prior to the actual switch closure since very small currents are involved and often the gap is not even bridged. The period following this, from the time of critical current formation to where the external circuit determines current flow, can be divided into two parts. First, is the establishment of streamers or canals that bridge the gap quite quickly. This time is extremely short, at least 10 times shorter than the lag time. Second, is the growth of the canal which is limited by its own inductance.

It will be assumed that the formation of the streamers does not constitute part of the closure time. The time for switch closure is thus assumed to be the time from when the canal has bridged the gap to when it is "fully" formed. Using a 10 percent to 90 percent criterion and assuming the growth to be limited only by the switch's inductance and the external circuit impedance, Z , the risetime t_r is given by

$$t_r = 2.2 \mathcal{L}/Z$$

using the fact that the current grows as

$$1 - e^{-t/(\mathcal{L}/Z)}.$$

The risetime, t_r , must be no greater than 1/4 cycle of the 1 GHz output for reasonably coherent output. This implies

$$\mathcal{L} \leq .114 Z \text{ nH.}$$

The inductance of the canal has been shown in Appendix B to go as

$$\mathcal{L} = 2 d(\text{cm}) \ln W_-/W_+$$

where W_- is the electron drift velocity and W_+ is the ion drift velocity.

Llewellyn-Jones⁽²⁰⁾ states that $W_-/W_+ \approx 10^2$. Thus,

$$\mathcal{L} \approx 9.2 d(\text{cm}) \text{ nH.}$$

Using this result, it is easy to see that

$$d \approx .0124 Z \frac{\text{cm}}{\Omega}.$$

The external circuit impedance, Z , is that of the transmission line formed by the device and is given by

$$Z = 377 \left(\frac{D}{W} \right) \Omega$$

where W is the width of the device.

Thus

$$d \approx 2D \approx .0124 (377) (D/W) \text{ cm}$$

and

$$W \approx 2.4 \text{ cm.}$$

e. Energy Storage Capabilities

The device dimensions are required to be

(1) $L = 15 \text{ cm}$

(2) $D = 1/2 \text{ cm}$

(3) $W = 2.4 \text{ cm}$

by frequency of operation, energy maximization, and switching times. The maximum E-field throughout the device is determined by the gas used, the pressure, and the requirement that breakdown be avoided while the pulse is exiting the device. The field was found to be

$$E = 7.6 \times 10^8 \text{ V/m}$$

when SF_6 at 100 atms. is used.

The energy stored is then given by

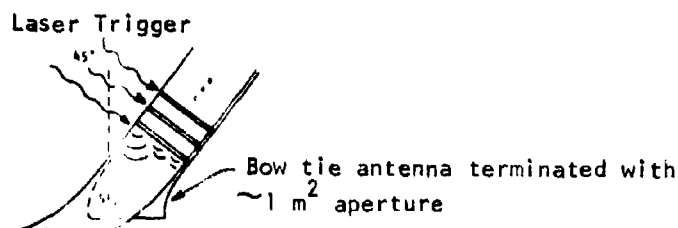
$$\begin{aligned} U &= \frac{1}{2} \epsilon_0 E^2 (10 \text{ LDW}) \\ &= \frac{1}{2} (8.85 \times 10^{-12}) (7.6 \times 10^8)^2 (10^1 \cdot 1.5 \times 10^{-1} \cdot 0.5 \times 10^{-2} \cdot 2.4 \times 10^{-2}) \\ &= 460 \text{ joules.} \end{aligned}$$

For a 1 m diameter aperture, the design requirements were modified to require only 100 joules at 1 GHz. Since only half the stored energy goes into the 1 GHz fundamental of the square wave pulse, the total energy storage requirement is 200 joules. This requirement is met by the device. The fact that D is so small cannot be allowed to interfere with the nearly uniform field of the gap. If the following configuration were used, this problem could be avoided.



f. Configuration

A possible configuration for this device is



The 45° cant is there to allow a laser beam to nonsynchronously fire the gaps with the resulting waveform entering the antenna synchronously. The horn shape is used so that the electric field strength will drop to the value that can propagate through air without breakdown. The antenna also provides a means of controlling the directivity of the output and provides an impedance match to free space. Since $\epsilon \cong \epsilon_0$ for SF_6 , the presence of this gas causes no impedance matching problems.

The entire system must be enclosed so that it can be pressurized. The enclosure should also be made to serve as a shield to prevent electromagnetic leakage. Further the antenna and enclosure could be divided into gastight, microwave transparent partitions, with progressively reduced pressures, lessening structural requirements. The pressure reduction is possible because, as the antenna cross section increases, the E-field decreases and less pressurization is required to prevent breakdown.

2. FROZEN B-FIELD DEVICE

a. Remote Switches

(1) Background

The output of the axial frozen B device into the outside air appears as follows when a single remote switch is employed.



Because of the large separations between half cycle square waves, an individual half cycle square wave can be treated as an individual pulse. The duration of this pulse for the two configurations in Section III was 0.5 ns and 33 ps and the maximum field strength will be greater than that derived in the section on Modified Design Requirement. Thus, this waveform will allow more peak power to be transmitted by the 1 m diameter aperture. However, the quantity that has the most significance is the average power.

(2) Power Output

Making use of Felsenthal and Proud's results (4) ~~once~~ again, it is found that

$$E_{MAX} \text{ (air, 1 atm, 0.5 ns)} \cong 95 \text{ kV/cm}$$

$$E_{MAX} \text{ (air, 1 atm, 33 ps)} \cong 300 \text{ kV/cm.}$$

This yields approximately 4 and 40 times the power, P_o , represented by 45.6 kV/cm that is obtained for air at 1 atmosphere with a 10 ns square wave pulse. However, this is peak power while the average power is much less. The average power is found by multiplying by the efficiency

$$P(0.5\text{ns}) = \left(\frac{95}{45.6}\right)^2 P_o \cdot 5.35 \times 10^{-2}$$

$$= 0.232 P_o,$$

$$P(33 \text{ ps}) = \left(\frac{300}{45.6}\right)^2 P_o \cdot \frac{2}{15}$$

$$= 5.77 P_o.$$

Thus, the $d_{12} = 1$ cm configuration would be superior to the frozen E-field device with respect to required antenna aperture size while the $d_{12} = 15$ cm configuration device would be inferior.

Since the two remote switch configurations have already been shown to have similar energy storage capabilities with respect to 1 GHz output potential, the $d_{12} = 1$ cm device is clearly superior to the $d_{12} = 15$ cm configuration. Only this configuration will be treated any further.

(3) Aperture Size and Energy Storage Requirements

While the $d_{12} = 1$ cm configuration would allow more average power to be transmitted from a 1 m diameter aperture than the frozen E-field device, this would require even more stored energy and, because of the device's small size, it is unlikely this energy could be stored. Instead, it will be assumed that the aperture is scaled down so that, at most, 100 joules can be radiated at 1 GHz just as was required for the frozen E-field device. The efficiency of 2/15 implies that 750 joules total energy must be stored.

(4) Device Geometry for Required Energy Storage

The maximum B-field allowed within the device will be determined for SF_6 at 100 atmospheres allowing meaningful comparison. The maximum E-field strength was found to be

$$E_{\text{MAX}} (\text{SF}_6, 100 \text{ atms}, 33 \text{ ps}) \cong 1 \times 10^9 \text{ V/m.}$$

The maximum allowed B-field is then

$$B_{MAX} = (\epsilon_0 \mu_0)^{1/2} E_{MAX}$$

$$= (3.33 \times 10^{-9}) (1 \times 10^9 \text{ V/m})$$

$$= 3.33 \text{ Weber/m}^2.$$

The current that must flow through a center conductor of radius $a = \frac{1}{4}$ cm, to provide this B_{MAX} at the surface of the conductor, is given by

$$I = \frac{2\pi a B_{MAX}}{\mu_0}$$

$$= \frac{\frac{1}{2} \pi 10^{-2} \cdot 3.33}{4\pi \times 10^{-7}}$$

$$= 0.416 \times 10^5 \text{ amps.}$$

This is well within the limits of a chemical generator.

The energy stored by the device is given by

$$U = \int_S \frac{1}{2} \frac{B^2}{\mu} dA \cdot L$$

$$= \iint \frac{1}{2} \left(\frac{\mu I}{2\pi r} \right)^2 \frac{1}{\mu} r d\theta dr \cdot L$$

$$= \frac{\mu I^2 L}{4\pi} \ln b/a$$

where A is the cross sectional area, L the length and b the radius of the outer cylinder. Requiring U = 750 joules, b is given by

$$\ln \left(\frac{b}{a} \right) = \frac{4\pi U}{\mu_0^2 L}$$

$$= \frac{4\pi \cdot 7.5 \times 10^2}{4\pi \times 10^{-7} (0.416)^2 \cdot 10^{10} \cdot 0.15}$$

$$= 28.9.$$

Therefore

$$b \approx \infty.$$

This is simply an impossible geometry to achieve from a practical standpoint.

The only way $\ln \left(\frac{b}{a} \right)$ can be reduced to where b is reasonable is to increase l or L. However L is fixed by the fact that the central conductor has 10 elements of length $d_{12} = 1\text{cm}$. l is fixed at 0.416×10^5 amps by breakdown considerations. It must be concluded that the required energy cannot be stored in a moderate sized device of this type.

b. Multiple Switches

(1) Background

For multiple switching, the maximum output field strength allowed by the outside air is just the same as for the frozen E-field device, since there is zero separation between half cycles. The device is required to deliver 100 joules from a 1 m diameter aperture at 1 GHz and, because of the square wave output, this implies a total output of 200 joules.

(2) Device Geometry for Required Energy Storage

In order to allow meaningful comparisons, the frozen B-device will be assumed to contain SF₆ at 100 atmospheres.

The maximum allowed E-field for SF₆ at 100 atmospheres is the same as for the frozen E-field device, namely

$$E_{MAX} = 7.6 \times 10^6 \text{ volts/cm.}$$

The maximum allowed B-field is then

$$\begin{aligned} B_{MAX} &= \sqrt{\epsilon_0 \mu_0} E_{MAX} \\ &= 3.33 \times 10^{-9} \cdot 7.6 \times 10^8 \text{ volts/m} \\ &= 0.253 \text{ Weber/m}^2. \end{aligned}$$

The current that must flow through a center conductor of radius $a = 1 \text{ cm}$, to provide this B_{MAX} at the surface of the conductor, is given by

$$\begin{aligned} I &= \frac{2\pi a B_{MAX}}{\mu_0} \\ &= \frac{2\pi \cdot 10^{-2} \cdot 0.253}{4\pi \times 10^{-7}} \\ &= 1.27 \times 10^4 \text{ amps.} \end{aligned}$$

This is well within the limits of a chemical generator.

The energy stored by the device is given by

$$\begin{aligned}
 U &= \int_s \frac{1}{2} \frac{B^2}{\mu} dA \cdot L \\
 &= \iint \frac{1}{2} \left(\frac{\mu I}{2\pi r} \right)^2 \frac{1}{\mu} r d\theta dr \cdot L \\
 &= \frac{\mu I^2 L}{4\pi} \ln \left(\frac{b}{a} \right)
 \end{aligned}$$

where b is the radius of the outer cylinder. Requiring $U = 200$ joules for the multiple switch device, the outer radius is found to be

$$\begin{aligned}
 \ln \left(\frac{b}{a} \right) &= \frac{4\pi U}{\mu I^2 L} \\
 &= \frac{4\pi \cdot 2 \times 10^2}{4\pi \times 10^{-7} \cdot (1.27)^2 \times 10^{10} \cdot 1.5 \text{ m}} \\
 &= .86.
 \end{aligned}$$

Therefore

$$\begin{aligned}
 b &= 2.36 a \\
 &= 2.36 \text{ cm.}
 \end{aligned}$$

The frozen B-device with multiple switches, as stated before, has similar storage capabilities to the frozen E-device but requires fast opening switches that may well be impossible to construct at present.

(3) Switch Considerations

In summary, the multiple switches used with the frozen B field device must do the following:

- (1) Must be opening switches for radiation to occur.
- (2) Time to open must be 250 ps or less for 1 GHz operation.
- (3) Synchronization between switches must be within 250 ps.

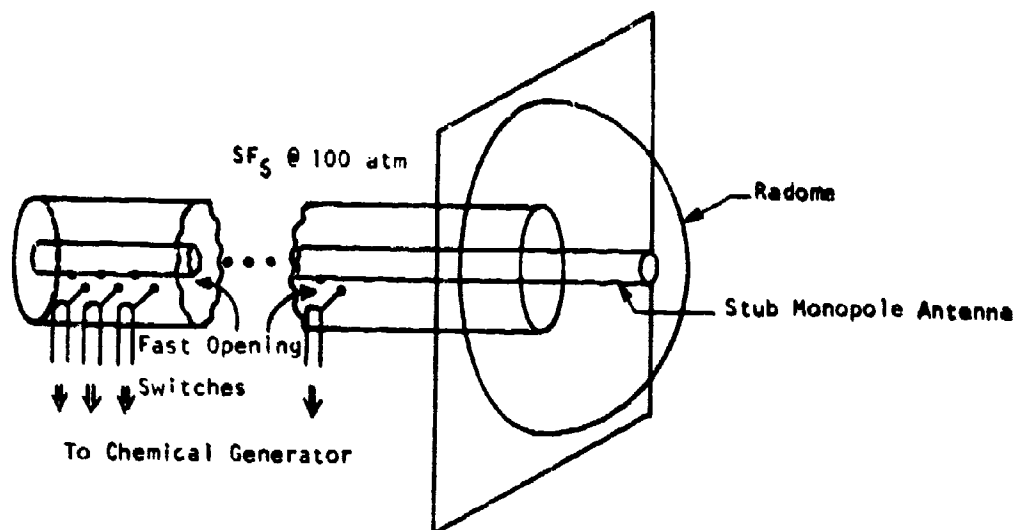
The last requirement is perhaps the hardest to satisfy. At present, no practical method of achieving the required synchronization appears to be available for the power levels under consideration. This statement is based on a survey of available literature, private communications (5), and an examination of the spread in times that occur when finely machined (10^{-4} cm) contacts are explosively separated.

While presently unavailable, the desirability of fast opening, synchronized, multiple switches is quite great. Any type of wave forming device working at frequencies > 1 GHz can make great use of such switches. In particular, any device using energy stored as the result of a quasi-static or static current flow requires opening switches to operate efficiently (see Sections III 2a.(6) and III 2.c.).

It is probable that when and if such switches can be developed a whole new set of technologies based on these switches will develop, just as several technologies now depend on the ability of spark gaps to provide fast closing, highly synchronized switching.

(4) Possible Configuration

A possible configuration for the multiple switch frozen B-field device, assuming fast enough opening switches could be constructed and synchronized is

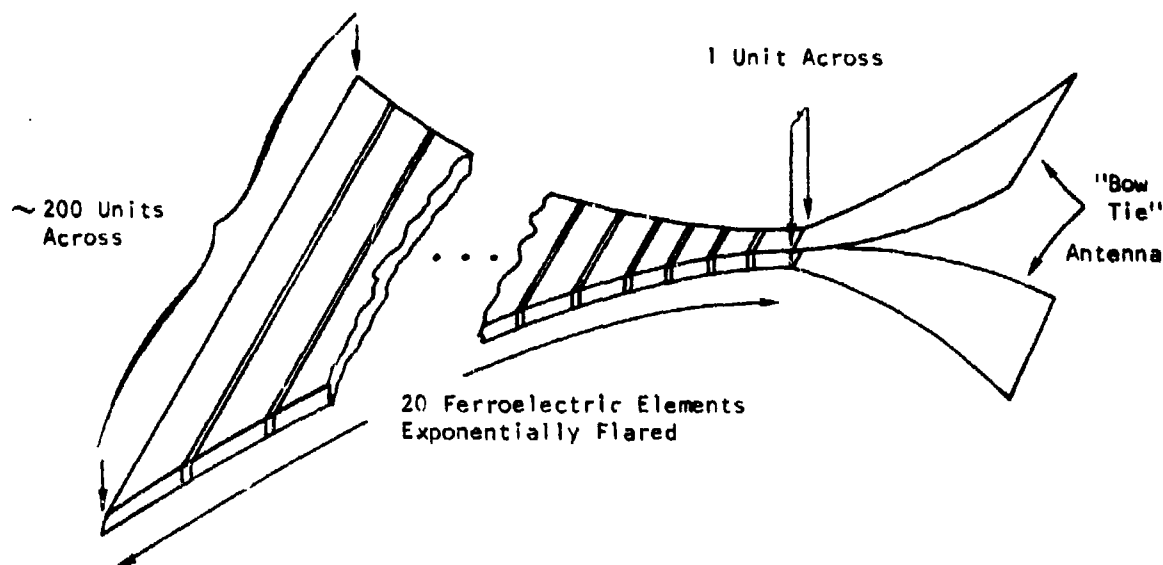


3. FERROELECTRIC DEVICE

a. Attenuation Loss Solution

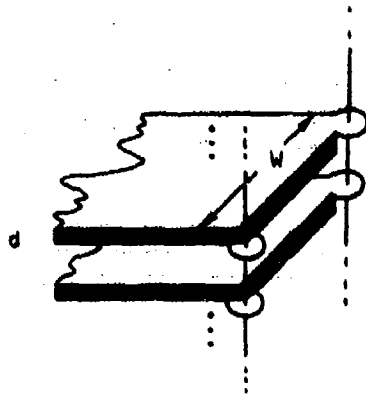
The main disadvantage of the ferroelectric device was the fact that the signal from the elements is progressively attenuated as they are located farther from the antenna. This can be rectified by scaling

the size of each element to compensate for the loss and by not attempting to use the backward traveling wave so that 20 elements must be employed. The device then looks as follows



b. Coupling Problems

There is still the problem of efficiently coupling the ferroelectric device to the antenna which has been taken as a "bow tie" antenna to keep the analysis simple. Let the individual "sandwiches" be connected in parallel as illustrated to achieve mechanical simplicity.



The impedance of an individual sandwich goes as

$$Z_{c \text{ sandwich}} = \sqrt{\frac{\mu}{\epsilon}} \frac{d}{W}$$

where d = separation and W = width of line element

Connected as shown in parallel, the impedance becomes

$$Z_{c \text{ element}} = \sqrt{\frac{\mu}{\epsilon}} \frac{1}{N} \frac{d}{W}$$

where N is the number of sandwiches in an element (same for all elements).

Since N is ~ 1000 , $\mu \approx \mu_0$, $\sqrt{\epsilon} \approx 30 \sqrt{\epsilon_0}$ and $d = 6 \times 10^{-4}$ cm, Z_c is extremely small. At the entrance to the antenna, the impedance can be approximated by that of a transmission line of equivalent dimensions. Taking the separation to be equal to the height of the element and the width to be the same as the element, while assuming the antenna to be air filled, yields

$$Z_{c \text{ antenna}} = \sqrt{\frac{\mu_0}{\epsilon_0}} \frac{Nd}{W}$$

This is $\sim 40 N^2$ greater than the element impedance and this mismatch is so extreme as to produce almost zero coupling. No method other than connecting

each sandwich to a small individual "bow tie" antenna using a quarter wave section with properly selected dielectric materials to obtain an impedance match appears to bypass this coupling problem. The mechanical difficulties of the individual antenna approach are immense considering the number required is $N \approx 1000$.

SECTION VI

CONCLUSIONS AND RECOMMENDATIONS

1. CONCLUSIONS

The conclusions drawn are:

- (1) A conventional chemical generator of current design will not produce significant 1 GHz output by itself.
- (2) Any intermediate device for frequency conversion of a conventional chemical generator's output must use nonlinear elements.
- (3) Nonlinear devices used by themselves with a chemical generator can result in little or no significant 1 GHz output.
- (4) Storage devices that:
 - (a) Store an appreciable fraction ($\sim 1/1000$ or more) of the chemical generators output,
 - (b) Use an array of resonant length elements,
 - (c) Employ nonlinear elements (i.e., switches),

can theoretically convert the stored energy to an appreciable output at 1 GHz. These devices are referred to as frozen wave devices.

- (5) A ~~nonconventional~~ generator using operating dimensions, d , such that d divided by explosively derived velocities, v , yields operating times, t , on the order of 1 nanosecond will have a small ($\sim 1/10$) portion of the output around 1 GHz and constitutes another possible approach.
- (6) Not all frozen wave devices will radiate appreciable amounts of energy. For example, the boundary conditions governing the slotted frozen B-field device leads to a nonpropagating component dominating the modal decomposition of the field so that after switching negligible energy is radiated.
- (7) Breakdown limitations imposed on the radiating pulse as it traverses a frozen E- or B-field device yield similar useful storage capabilities of the frozen E- and B-field devices.
- (8) Breakdown limitations on the pulse after entering the surrounding air limits the energy that can be radiated from a 1m^2 aperture to ~ 100 joules at 1 GHz (200 joules total for a square wave pulse train) for a 10 cycle pulse at altitudes of ~ 5 km and to even lesser amounts as altitude increases.
- (9) Because of (8) a modification to the RADC requirements was made. A power level of 10^{10} watts and an energy radiated of 100 joules, assuming a 1m^2 aperture, became the requirement for operation above ~ 5 km.
- (10) Three device types were found to offer some promise of meeting the design requirements. They were
- (a) Frozen E-field device.

- (b) Axial frozen B-field device.
- (c) Ferroelectric device (this device made use of small operating size).
- (11) The frozen E-field device, using 1 cm gaps, 1/2 cm plate separation, 2.6 cm plate width insuring 1/4 ns switch times, pressurized with SF₆ at 100 atmospheres and assuming high power UV triggering of the gaps, can store and transmit 460 joules with 230 joules at 1 GHz assuming no losses. Further, the low jitter times (~0.1 ns) possible with UV laser triggering would allow several such devices, which are compact, to be operated in parallel, resulting in much higher power levels that could be used below ~5 km.
- (12) The axial frozen B-field device could be operated in two modes, with a single remote switch or multiple in-place switches. The single remote switch resulted in markedly lower efficiency or storage capabilities depending on design parameters in comparison to the frozen E-field device. The multiple switch mode had comparable efficiency and storage capabilities in comparison with the frozen E-field device. However, both device modes require fast opening switches. For the multiple switch mode synchronization requirements exceed state-of-the-art capabilities.
- (13) The ferroelectric device had a significantly lower efficiency than the frozen E-field device because of the lossy nature of the ferroelectric material, BaTiO₃. Coupling the device efficiently to an antenna was found to be difficult. One efficient method is to terminate each individual "film" of BaTiO₃ with an ultrasmall bow tie antenna using a quarter wave

section between them for impedance matching at 1 GHz. This represents a very formidable fabrication problem.

(14) Other devices:

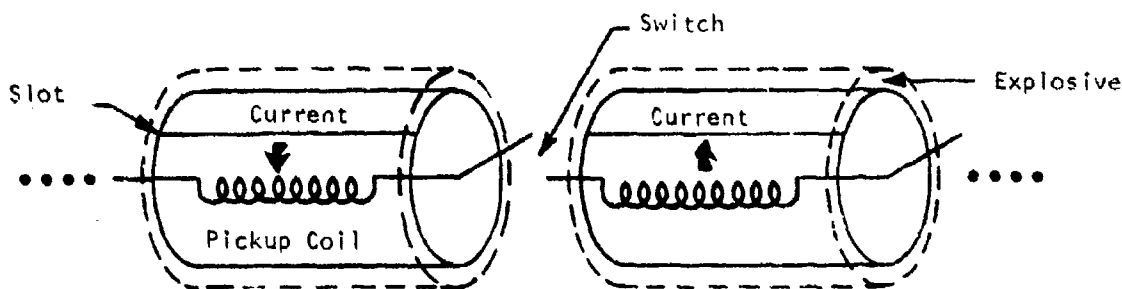
Several novel approaches using the output of a conventional chemical generator were tried and not found promising. The problems encountered with each approach can be summarized as follows:

- (a) Moving Mirror - Only single reflection available, needed velocity cannot be obtained chemically. For plasma "mirror" very large particle accelerator needed.
- (b) Compressed Cavity - Too large for nominal 1 MHz initial input ($\sim 100\text{m}$). Chemical compression times too long in that losses become excessive.
- (c) Cavity with Expanding Plasma - Too large, compression ratio available not large enough. Faster operation than compressed cavity with less losses.
- (d) Plasma Oscillation - Too large.
- (e) Raman & Brillouin Scattering - Can't excite high enough modes strongly enough to provide useful coupling.
- (f) Synchrotron Radiation - Most sophisticated approach is still over four orders of magnitude too low in terms of energy produced. However, there is some possibility of improved performance using the megagauss fields available from chemical generators.
- (g) Capacitive/Inductive Discharge - Doesn't radiate.

2. RECOMMENDATIONS

Recommendations are as follows:

- (1) Further study of frozen wave devices be performed. Not all possible configurations have been examined. For example consider the following configuration as a possible candidate for further study.



The outer cylinders are slotted so that alternating azimuthal currents can be impressed around the cylinders by an outside source, generating small alternating axial B-fields. The cylinders are then explosively compressed generating intense B-fields linking the inner "pickup" coils. When dB/dt is a maximum and at this point the switches can be closed with alternating currents resulting along the central conductor formed by the pickup coils. The efficiency of such a procedure remains to be determined.

- (2) Further study of novel device types. Not all the possibilities could be examined in the time allocated.
- (3) Fast acting nonlinear devices, other than spark gaps which are reasonably well understood, should be studied so as to obtain a good theoretical understanding. This will allow future investigators to determine their applicability in frequency

converting the output of a conventional chemical generator. In particular, more work is needed on fabricating and understanding fast opening switches.

- (4) A detailed study of power limitations imposed by breakdown considerations is needed. In the work presented in this study, beam divergence, free electron density fluctuations, free electrons generated by moving aircraft, and a variety of other complicating factors have not been considered.

REFERENCES

- (1) Crawford, J. C. and R. A. Damerow, "Explosively Driven High-Energy Generators," J. Appl. Phys., Vol. 39, No. 11, 1968.
- (2) Houston, S., "Hertzian Generator Development," BDM/A-90-73-TR, August 1973.
- (3) Bettis, J. R., and A. H. Guenther, "Subnanosecond-Jitter Laser-Triggered Switching at Moderate Repetition Rates," IEEE J. of Quant. Elec., Vol. QE-6, No. 8, 1970.
- (4) Felsenthal, P. and J. M. Proud, "Nanosecond-Pulse Breakdown in Gases," Phys. Rev., Vol. 139, No. 6A, 1965.
- (5) Private Communication with Dr. A. S. Gilmour, Jr., SUNY at Buffalo.
- (6) Furth, H. P., et al, "Production and Use of High Transient Magnetic Fields," II, Rev. Sci. Inst., Vol. 28, No. 11, Nov. 1957.
- (7) Kittel, C., Introduction to Solid State Physics, 3rd edition, Wiley, 1963.
- (8) Fatuzzo, E. and W. J. Merz, Ferroelectricity, Vol. VII of Selected Topics in Solid State Physics, ed. E. P. Wohlfarth, Wiley, 1967.
- (9) Samora, G. A., "The Effects of Hydrostatic Pressure on Ferroelectric Properties," J. Phys. Soc. Jap., Vol. 28, Supplement, 1970.
- (10) Montgomery, D. C. and D. A. Tidman, Plasma Kinetic Theory, McGraw-Hill, 1964.
- (11) Jackson, J. D., Classical Electromagnetics, Wiley, 1962.
- (12) Glasston, S. and R. H. Lovberg, Controlled Thermonuclear Reactions, Van Nostrand, 1960.
- (13) Granastein, V. L., et al., "Coherent Synchrotron Radiation from an Intense Relativistic Electron Beam," NRL Memorandum Report 2706, (Jan. 1974).
- (14) Yariv, A., Quantum Electronics, Wiley, 1967.
- (15) Pantell, R. H. and H. E. Puthoff, Fundamentals of Quantum Electronics, Wiley, 1969.
- (16) Nesterikhin, Y. E., et al., "Pulsed Breakdown of Small Gaps in the Nanosecond Range," Sov. Phy.-Tech Papers, Vol. 9, No. 1, 1964.

REFERENCES (Continued)

- (17) Morse, P. M. Thermal Physics, Benjamin, 1965.
- (18) Messler, Capt. M. A., "The Ionospherically Propagated Exoatmospheric EMP Environment," EMP Theoretical Notes, Note 163, 1972.
- (19) "Nanosecond Pulse Breakdown (U)," Tech. Doc. Rep. No. RADC-TDR, November 1965.
- (20) Llewellyn-Jones, F., Ionization and Breakdown in Gases, Wiley, 1957.
- (21) "High Power Travatron Investigation (U)," Tech. Rep. No. RADC-TR-73-222, 1973.
- (22) Martin, J. C., "Nanosecond Pulse Techniques (U)," U.K.A.E.A., A.W.R.E. Tech. Memo SSWA/JCM/704/49, 1970.

BIBLIOGRAPHY

- Llewellyn-Jones, F., Ionization Avalanches and Breakdown, Methuen, 1967.
- Physics of High Energy Density, Proceeding of the International School of Physics "Enrico Fermi," Course XLVIII, ed. P. Caldirola and H. Kneepfel, Academic Press, 1971.
- Kneepfel, Heinz., Pulsed High Magnetic Fields, North-Holland, 1970.
- Jordan, E. G. and K. G. Balmain, Electromagnetic Waves and Radiating Systems, 2nd Edition, Prentice-Hall, 1968.
- Zel'dovick and Raizer., Physics of Shock Waves of High Temperature Hydrodynamic Phenomena, Vol. I and II, Academic Press, 1967.
- Churchill, R. V., Fourier Series and Boundary Value Problems, 2nd Edition, McGraw-Hill, 1963.
- Bracewell, R., The Fourier Transform and Its Applications, McGraw-Hill, 1965.
- Fowler, C. M., W. B. Garn, and R. S. Caird., "Production of Very High Magnetic Fields by Implosion," J. Appl. Phys., Vol. 31, No. 3, 1960.
- Shears, J. W., et al., "Explosive-Driven Magnetic-Field Compression Generators," J. Appl. Phys., Vol. 39, No. 4, 1968.
- Herlach, F., "Flux Loss and Energy Balance in Magnetic Flux-Compression Experiment," J. Appl. Phys., Vol. 39, No. 11, 1968.
- Cummings, D. B., "Cascading Explosive Generators with Autotransformer Coupling," J. Appl. Phys., Vol. 40, No. 10, 1969.
- Lockwood, D. L., "Pulsed Vacuum Arcs," Doctoral Dissertation in Elec. Eng. at SUNY (Buffalo), 1973.
- Pease, M. C., "Energy Conversion Techniques for Microwave Generation (U)," Tech. Rep. No. RADC-TR-65-254, 1965.

APPENDIX A

OVERVOLTED FROZEN E DEVICES

In the article (4) by P. Felsenthal and J. M. Proud the breakdown lag times for short electric pulses were presented. These results will be used in this section to derive, based on a plausible assumption, the amount by which the capacitive E-field device can be dynamically overvoltage and still be operator switched avoiding self-breakdown.

A chemical generator with a peaking circuit is capable of producing far in excess of the breakdown field strength in the 1 usec of operation in which the current rises approximately linearly to a maximum. This is based on the assumption that breakdown at these extreme voltages could somehow be prevented and on the energy output capabilities of the generator and the E-field device energy storage volume. In reality, breakdown will occur before these field strengths are reached. However, it is possible to very conservatively characterize the rate of E-field change available by

$$\begin{aligned}\frac{dE}{dt} &> \frac{100E_B}{10^{-6}\text{sec}} \\ &= \frac{10^8 E_B}{\text{sec}}\end{aligned}$$

where E_B = breakdown strength of air at 1 atm.

The assumption that will be made for the derivation is that one is assured of reaching $E(t)$ where $E(t) > E_B$ without breakdown if

$$\tau \leq t_0[E(t)] + t \text{ for all } t \leq \tau$$

and if $E(t)$ is a monotonically increasing function of time. That is, the system will reach a field strength $E(t) = E_b$ at time t , provided that at any intervening time t , the electric field has an associated lag time t_l that added to t gives a time greater than or equal to t .

Based on this assumption, the maximum E one is assured of reaching without breakdown occurring is $E_{\max} = E(t_{\max})$ where

$$t_{\max} = t_l [E(t_0)] + t_0 = t_{l_0} + t_0$$

and $t_{l_0} + t_0$ is the minimum value $t + t_l$ assumes. That this minimum exists is shown by the fact that just above breakdown t_l is relatively large and very rapidly diminishes with increasing field. Thus $t_l + t$ initially drops, while for very large t , $t_l + t \rightarrow t$.

The time, t_0 , and from it, t_{\max} and E_{\max} , is found by setting

$$d\{t_l[E(t)] + t\}/dt = 0.$$

From Felsenthal and Proud

$$t_l = \frac{K}{k(E/p)}$$

where

$$K = \frac{\ln(n_b/n_0)}{p(\alpha/p - \beta/p)} = \frac{\ln(n_b/n_0)}{(\alpha - \beta)}, \quad k(E/p) = C_1 + C_2 E/p.$$

so that $d\{t_l + t\}/dt = 0$ leads to

$$1 + \frac{dt_l}{dt} = 0$$

with

$$\frac{dt_l}{dt} = K \frac{d}{dt} \left(\frac{1}{k(E/p)} \right) = -1$$

$$= \frac{-KC_2}{p[k(E/p)]^2} \frac{dE}{dt}.$$

Thus

$$1 - \frac{KC_2 (dE/dt)}{p[k(E/p)]^2} = 0.$$

From this E_0 , the electric field at t_0 , is found to be

$$E_0 = \left[\frac{Kp (dE/dt)}{C_2} \right]^{1/2} - \frac{C_1 p}{C_2}.$$

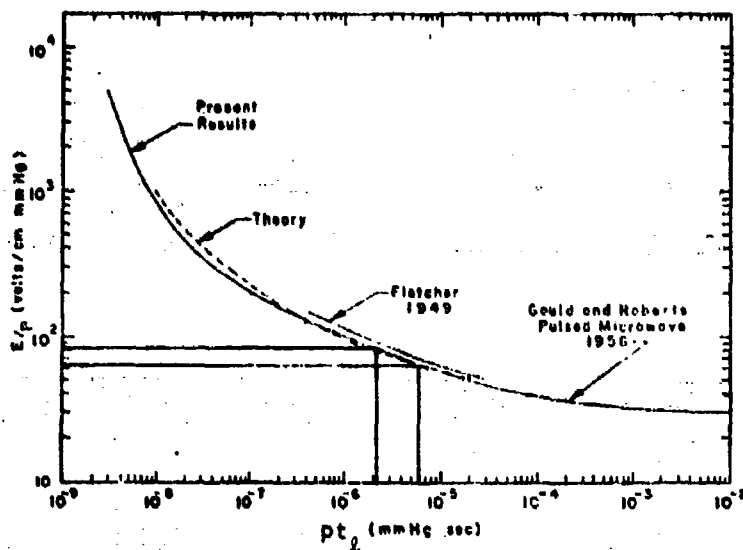
E maximum is then given by

$$\begin{aligned} E_{\max} &= E(\tau_{\max}) \\ &= E(t_0 + t_{l_0}) \\ &= E(t_0) + \int_0^{t_{l_0}} (dE/dt) dt \\ &= E_0 + \frac{\Delta E}{\Delta t} t_{l_0} \text{ for constant } dE/dt. \end{aligned}$$

It is possible to obtain E_{\max}/p for air from Figure 2 of Felsenthal and Proud's article by noting the following:

When an increase in E/p in time Δt above t results in a reduction in lag time, t_l , by an amount equal to Δt , the minimum in $(t_l + t)$ is determined. The time t corresponds to t_0 at this point and $E/p = E_0/p$.

Graphically this point can be found on the E/p versus $p t_l$ diagram. Assume $p = 760 \text{ mm Hg}$ and $dE/dt = 10^8 E_B/\text{sec} = 3 \times 10^{12} \text{ V/cm-sec}$. Then in $\Delta t = 5 \text{ ns}$ have $\Delta E/p = 20 \text{ V/cm-mm}$. If $\Delta t = 5 \text{ ns}$, must have $\Delta p t_l = 3.8 \times 10^{-6}$. Requiring the two conditions be met simultaneously yields, as shown below, $E/p = 72 \text{ V/cm-mm}$, thus $E_0 = 55,000 \text{ volts/cm}$.



The formative time for E_0 is

$$\tau = \frac{4 \times 10^{-6} \text{ mm sec}}{760 \text{ mm}}$$

$$\approx 5 \text{ ns.}$$

In this time period the field has risen by $E_B/2$. Therefore

$$E_{\text{max}} = E_0 + E_B/2$$

$$= 70,000 \text{ volts/cm.}$$

Since $\left(\frac{E_{\text{max}}}{E_B}\right)^2 = 5.7$, the operator switchable energy is easily five times greater than if the field were kept just below breakdown.

If nitrogen were used instead of air, the formula for E_0 is simplified considerably since from Felsenthal and Proud's data $C_1 = 0$. Thus E_0 for nitrogen increases as $p^{1/2}$. Note too that E_0 goes as $(dE/dt)^{1/2}$ so that a faster charging rate than assumed would yield higher values of E_0 and hence a higher value for E_{max} .

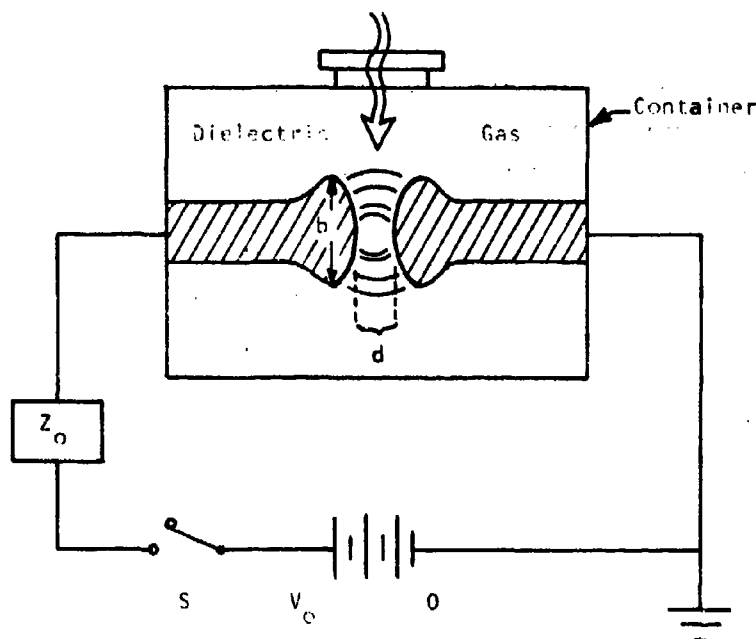
APPENDIX B

SPARK GAP TIME BEHAVIOR AND ITS MODELING

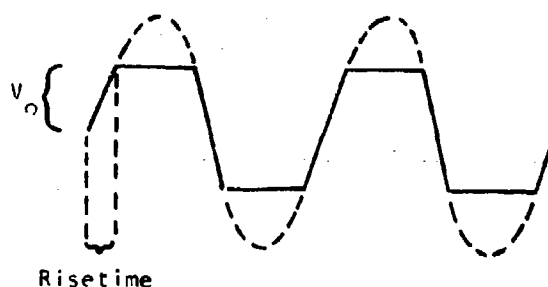
The electrical breakdown of a spark gap has been studied to gain a theoretical understanding of the basic physical processes and for the purpose of making better spark gaps. The intent here is to outline the basic processes involved and with that understanding, construct a model for spark gaps. The applied interest in spark gaps arises from the fact that they can be switched very quickly (under 1 ns) and carry large-current loads (once breakdown is completed, a spark gap behaves much like a section of line short circuiting the gap).

A concrete model of the physical apparatus will be used to keep the discussion well grounded. A minimal number of parts and a few simplifying assumptions result in the following picture:

Optional UV Laser or Other Source



A voltage source (in the diagram it is a battery, but it could be any type of power supply or even an oscillating source) is used to impress voltage V_0 across the gap. For unambiguous results in theoretical research, the voltage is applied with as fast a risetime as possible. In many practical applications, it is desirable to impress a large voltage, greater than the breakdown voltage, across the gap. If this is to be done, the voltage must rise to this value more quickly than the breakdown lag times encountered. Again, fast risetime is needed. It can be obtained with a switch, typically another spark gap, as shown in the diagram. Alternately, the voltage source could be oscillatory with the output clipped thusly

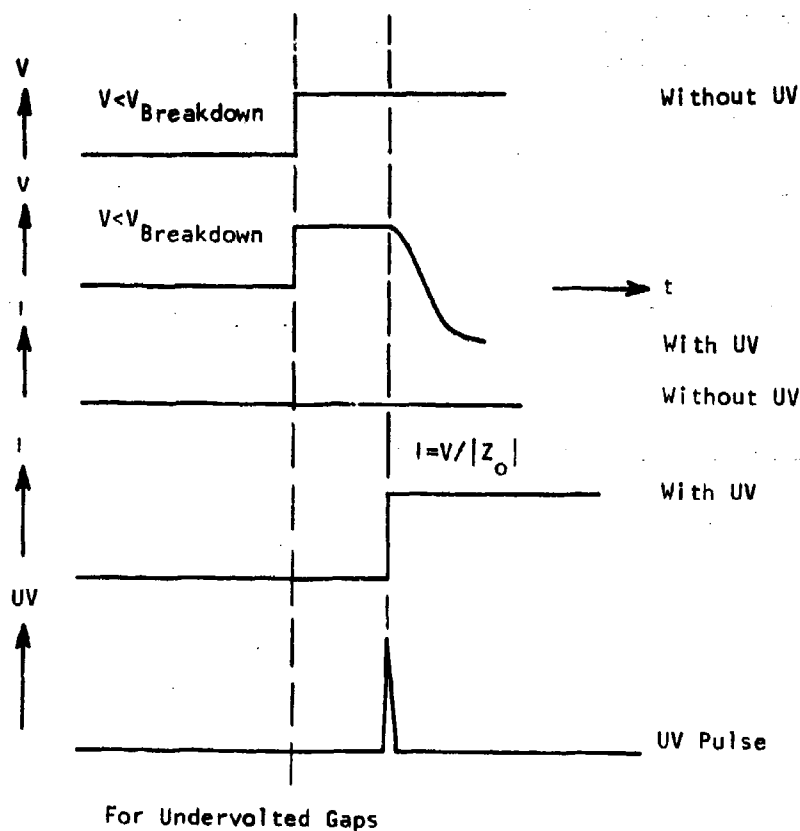


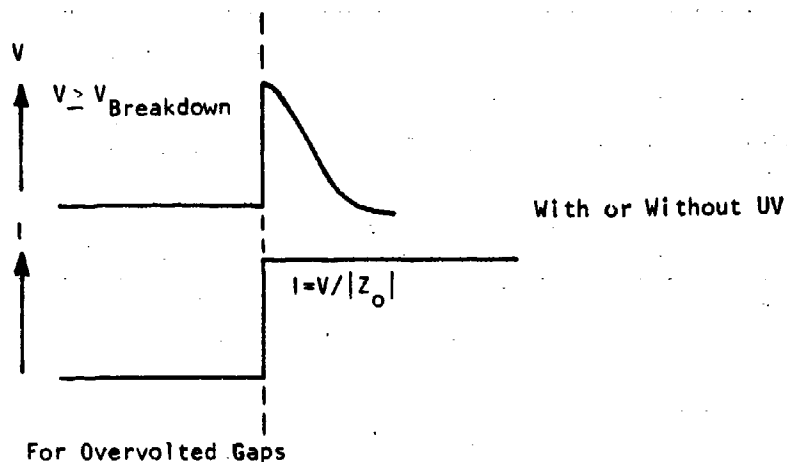
The statement that the source voltage impresses a voltage V_0 across the gap depends upon the fact that virtually no current flows across the gap initially. Thus, there is initially no voltage drop across the circuit's impedance Z_0 .

If the voltage V_0 is less than some voltage, called the breakdown voltage, V_B , the gap will not break down unaided. However, a laser beam operating in the UV, or any strong UV source or radioactive source, can initiate breakdown even when the gaps are below the breakdown voltage. The presence of a port for admitting UV radiation is shown as an option.

If the voltage is greater than the breakdown voltage, then breakdown will occur whether or not UV illumination is present. Once the breakdown process is complete, there exists a highly conducting ionized channel between the gaps. This channel can be modeled as a piece of wire connecting or shorting the gaps.

A spark gap model constructed at this level would look like





Zero risetime is used since no detailed understanding of the process is available at this level.

Breakdown occurs because a few free electrons in the gap (provided by the gas or by the metal electrodes) are accelerated by the applied voltage, strip off other electrons, and lead to an electron avalanche that bridges the gap. This spark channel then grows to a fixed size and breakdown is completed. The initial electrons are provided by thermal energy, cosmic rays, or by UV illumination. While this is a gross simplification, it provides a starting point from which to expand and clarify the basic ideas.

The electric field across the gap, not the impressed voltage V_o , determines electron acceleration. The gaps in our diagram are assumed to be in the Rogowski configuration so that the field is nearly uniform between the gaps and given by

$$E = V_o / d$$

It is experimentally observed that the breakdown voltage is related strongly to the gap spacing. Paschen's law states that the breakdown potential V_B is related to the product pd , where p is the pressure, by

$$V_B = f(pd)$$

Generally, for other than very low pressures where the collision frequency is quite low, V_B goes up linearly with pd . For fixed pressure, then, V_B goes up linearly with d . Clearly this just maintains a constant electric field strength. If one were to try to theoretically determine the breakdown voltage for a particular configuration, a first step would be to find the mean collision time of free electrons in the gas, then require the energy imparted to the electron by the electric field in this time to be equal to the ionization potential of a gas molecule so that an average collision would free another electron, and, from this required field strength, obtain the voltage. This would be a crude approximation since only a fraction of the collisions, which are statistically distributed in energy, need to free further electrons to yield an avalanche. Further, other processes are involved in producing electrons than just direct electron-molecular ionization. These additional processes include photoionization, multiple collision ionization, ion-molecule collision ionization, etc. As a result, most breakdown voltages are found experimentally and the results extended, if need be, by Paschen's law.

If no initial electrons are present, the growth of the avalanche for a system above the breakdown potential (i.e., overvolted) will show the very statistical nature of the breakdown process in that there will be a noticeable variation in the time it takes to reach a well developed stage of avalanche growth. This is because there will be a spread in time from experiment to experiment of how long it takes the necessary initiatory electrons to appear to start the avalanche process off. The Russians (16) further claim that even if a few initiatory electrons are present, these do not always lead to an avalanche that goes to completion of breakdown, rather

that the avalanche may be quenched and another started and so on until one goes to completion. The variation in time it takes the avalanche to become developed well enough to lead to complete breakdown is referred to as jitter.

For undervolted systems without illumination, an avalanche never gets well developed. Actually, there is a very small statistical probability that a sufficient number of free electrons will appear as the result of statistical fluctuations and that an avalanche will go to completion. The use of a UV laser can force these electrons to appear. However, if the voltage is far below breakdown, even this may not insure breakdown.

For systems just below the breakdown voltage with nonuniform fields, a steady state condition occurs in which the space about the electrodes glows. This is the result of ionization being exactly matched by recombination, leaving an ionized portion of the gas about the electrodes. This is referred to as a corona discharge.

The number of initiatory electrons typically available within a gap N_0 , is on the order of 10^1 corresponding to current $I_0 = 10^{-12}$ A. Under the influence of the electric field, these electrons are accelerated, collide with the gas molecules present, and ionize a portion of them, thereby generating more free electrons. This is the primary process by which electrons are generated. Secondary processes such as photoionization, in which photons generated by collisions impact the cathode and gas molecules, freeing additional electrons, also contribute.

The primary process results in an avalanche that grows as

$$I = I_0 e^{\alpha x}$$

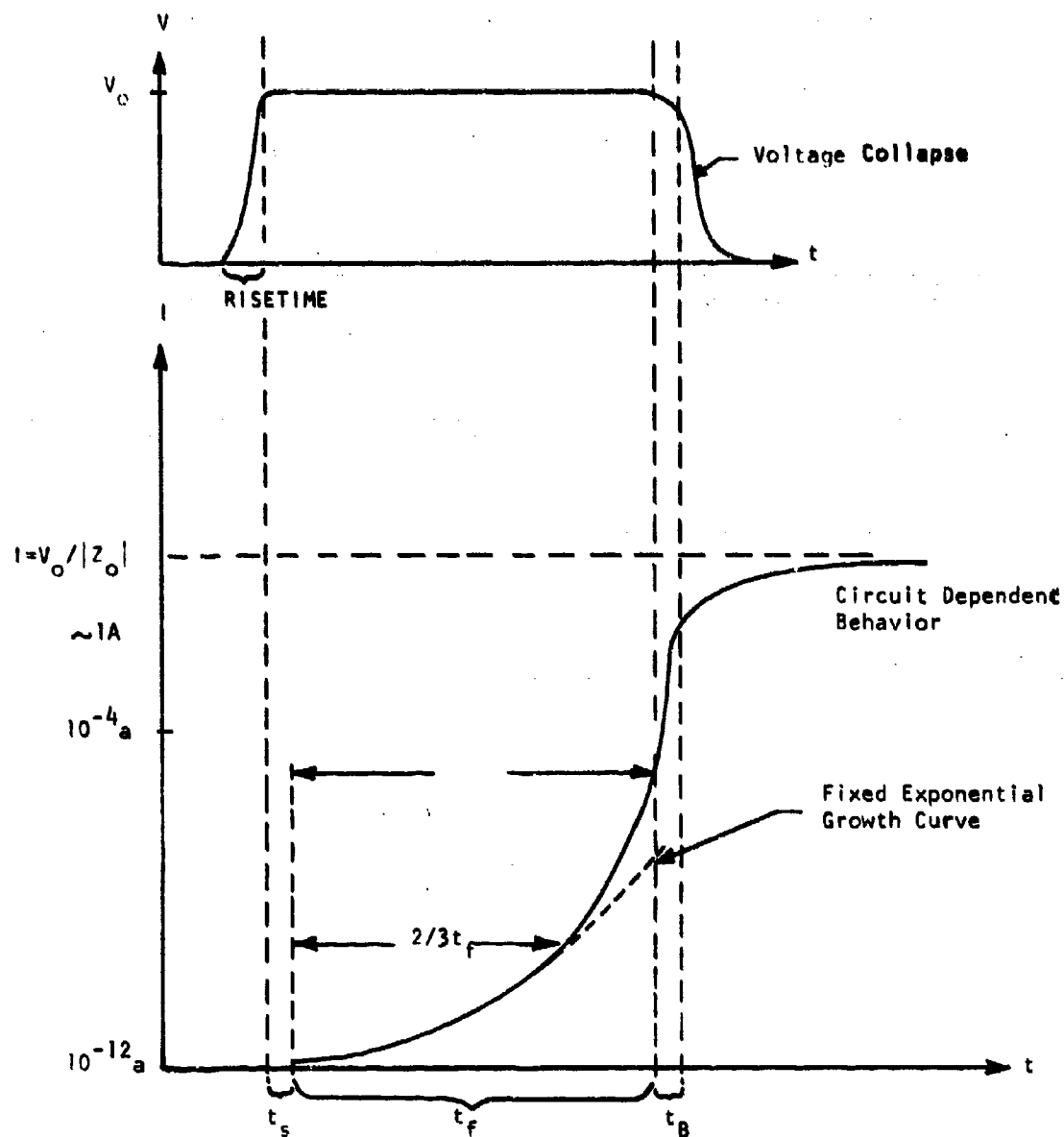
where α is the first Townsend coefficient which characterizes the primary process current. A critical current is reached when $I = I_c = 10^{-4}$ A corresponding to $N_c = 10^9$ electrons for a ratio of N_c/N_0 of 10^8 (4). This can occur

in a time less than the transit time of an electron, t_e , the time it takes an electron to cross the gap (i.e., $t_e = d/W_e$ where W_e is the electron drift velocity). At this point, the secondary processes have become appreciable and the current growth exceeds the exponential growth rate given by $e^{\alpha x} = e^{\alpha W_e t}$. The period of time from the application of the voltage to when the current reaches this critical value is called the breakdown lag time or the delay time.

The breakdown lag time for many different gases has been experimentally determined, along with theoretical predictions that closely match experiments by Felsenthal and Proud (4). Their results are graphically displayed in this reference. Llewellyn-Jones (2) has stated that for approximately 2/3 of the delay time (which he calls the formative delay time) the current growth is given by a fixed exponential, after that, secondary processes account for the increased growth rate in the last third of the delay time.

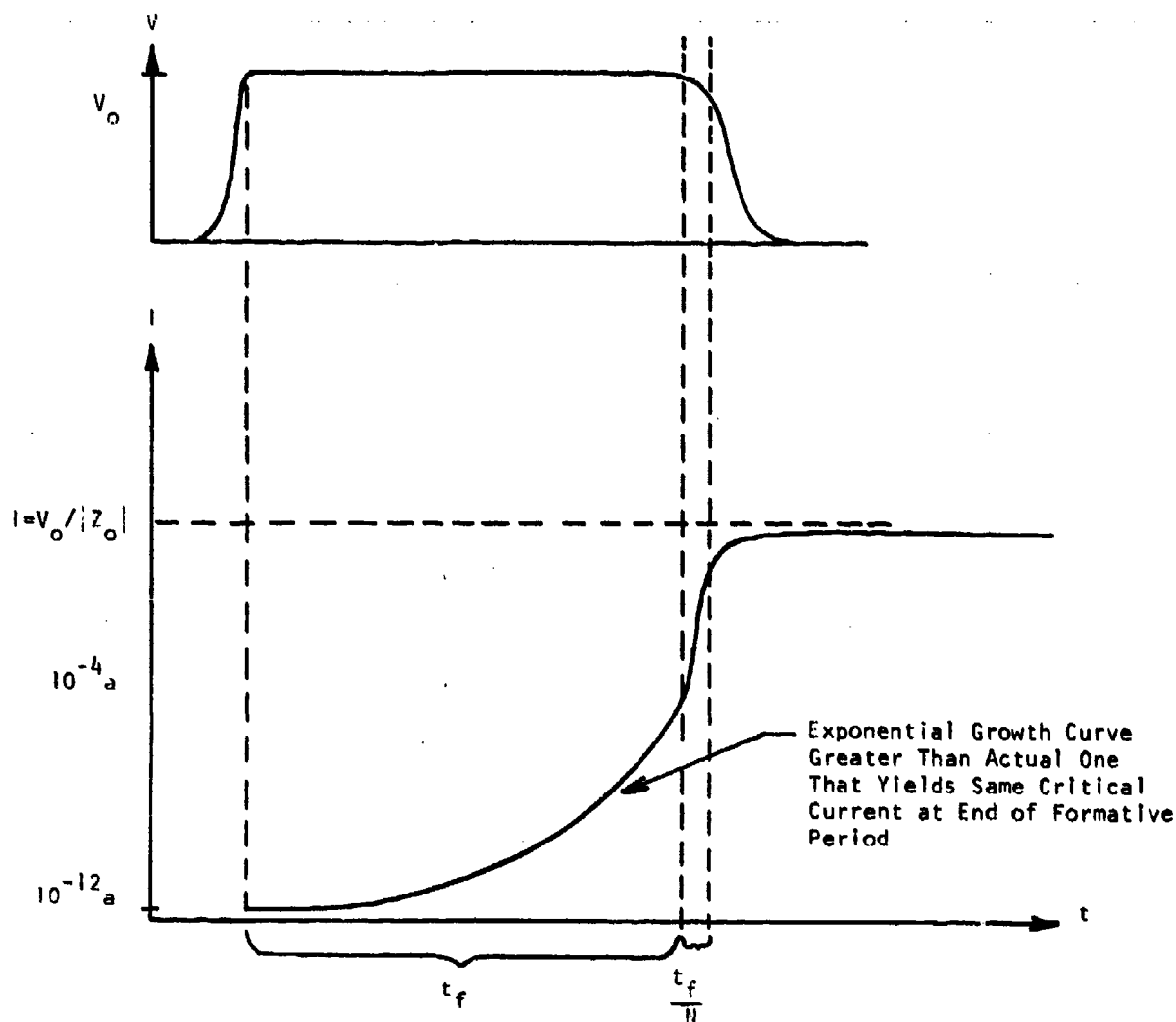
When the current has reached this critical value, breakdown has not been completed. No appreciable drop in the voltage across the gap has occurred, nor, in some cases, have the electrons bridged the gap. The completion of breakdown takes place from the time the critical current is reached to when a voltage collapse commences. This time is extremely short, according to some Russian investigators (16) at least an order of magnitude less than the lag time. One proposed mechanism is that canals or streamers are formed in which the electrons move with vastly greater W_e 's to complete the bridging of the gap or to expand the spark from a small filament to a large one. Llewellyn-Jones alternately argues that the coefficients, such as α , describing the growth increase at this point accounting for the fast completion of the breakdown.

The various stages in the breakdown process for an overvolted system can be graphically displayed as

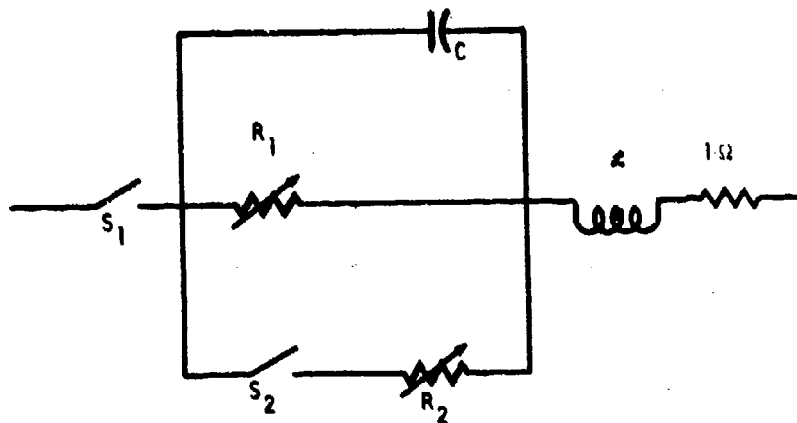


For a UV illuminated gap, t_s , the statistical delay time that accounts for the time it takes for initiatory electrons to appear on a statistical basis goes to virtually zero for a strong UV pulse.

A model of the behavior of an overvoltage gap (ignoring t_s so that it can be UV illuminated or not) is given by



In a circuit analog model, this behavior is given by the following set of circuit elements*



with the following sequence of events and circuit parameters:

parameters

$$R_1 = R_0 e^{-k(t-t_1)} U(t-t_1)$$

where $R_0 = \frac{V_0}{I_0}$ and $k = 18.4/t_f$ (provides 10^8 increase in I in t_f).

$$R_2 = \frac{R_0}{10^8} \left[(t_1 + t_f) + \frac{t_f}{N} - t \right] / \frac{t_f}{N}$$

$$\times U \left[t - (t_1 + t_f) \right] \times U \left[(t_1 + t_f(1 + \frac{1}{N})) - t \right]^{\sim}$$

where N = fraction of t_f breakdown completion occurs in and U is the Heaviside function.

$$C = \epsilon A/d = 2\pi\epsilon b^2/d$$

$$L = 2d \ln(W_-/W_+)$$

* It will be assumed that very fast switching is desired. The avalanche will not have bridged the gap before the critical point is reached so that the gap represents a capacitance at least up to this point when S_2 is closed shunting current around C .

\mathcal{L} is the inductance of a coaxial model of the spark when the ion filament forms the central conductor and the electron filament is modeled as the outer conducting sheath. This model is used in Reference (21) while a similar model is used in Reference (22). The 1Ω resistor represents an upper limit to the residual resistance after breakdown is completed. This is only a rough estimate.

- (1) S_1 and S_2 open.
- (2) S_1 closes at t_1 . For multiple switches t_1 becomes $t_1(n)$ where n is the switch number. With jitter present $t_1(n) \neq t_1(m)$ in general.

The current increases exponentially at a rate that yields the critical current in time t_f because of the exponential fall in the resistance R_1 . This is insured by selecting the decay constant k equal to $18.4/t_f$ and finding t_f from Reference (4) or other appropriate sources such as Reference (16). It is assumed that the initial current is that given by one electron crossing the gap at a velocity given by the drift velocity W_- . The capacitance C is negligible with respect to R and does not markedly affect the current growth.

- (3) At time t_f after S_1 closed (i.e., $t = t_1 + t_f$), the critical current is reached and breakdown occurs in a short time period after, given by t_f/N where $N \geq 10$. This is modeled by closing S_2 at $t = t_1 + t_f$, putting a linearly time varying resistance R_2 , in parallel with R_1 , that equals R_1 at $t = t_1 + t_f$ and goes to zero, shorting this segment of the circuit, in time $t = t_1 + t_f + t_f/N$.
- (4) Only \mathcal{L} and R remain to describe the spark gap. The growth of the spark is essentially determined by the external impedance and the spark inductance.

APPENDIX C

LASER TRIGGERED SWITCHING

Laser triggered switching (LTS) has been studied at the Air Force Weapons Laboratory (AFWL), Kirtland Air Force Base. In their paper(3), Bettis and Guenther show that a UV laser can provide subnanosecond jitter for a 1 cm gap. The gap was filled with 90 percent Ar - 10 percent N₂. Pure SF₆ was not used since higher laser powers would be required to produce a large enough number of free electrons to initiate low jitter breakdown. This follows from the fact that SF₆ is much more electronegative than Ar. However, using sufficient laser power, results similar for the 90 percent Ar - 10 percent N₂ mixture should hold for SF₆.

It was found that jitter as low as ~0.1 ns with ~10 MW could be obtained with a 1 cm gap with 90 percent Ar - 10 percent N₂ at 2925 torr and the gap at 90 percent of the breakdown potential. Under the same conditions the delay was found to be 4.5 ns.

The delay time does not represent the switch closure time. It is the time from the onset of the laser pulse to the onset of breakdown. The onset of breakdown is the time when an avalanche has reached its critical magnitude. At this point the current has grown to $\sim 10^{-3}$ A/cm² from a starting point of $\sim 10^2$ electrons. At the onset of breakdown it has been postulated that streamers or canals are established and the time to bridge the gap and begin the voltage collapse occurs in a time at least one order of magnitude smaller than the delay time according to a Russian paper(16). Lewellyn Jones(20) points out that the behavior of the current follows an exponential law for about 2/3 the delay time. It then grows at an ever faster pace completing breakdown shortly after the onset of breakdown. He states that rather than canals or streamers being formed, the coefficients

representing the various ionization processes responsible for the growth no longer remain constant and their increase accounts for the rapid completion of breakdown.

By the completion of breakdown, Llewellyn-Jones means the time to bridge the gap and begin the voltage collapse. Since the voltage is just starting to drop so that negligible energy has been transferred, this time can be considered as the beginning of switch closure. Switch closure will take place in a time determined by the spark inductance and the external impedance as can be seen from the model in Appendix B. Breakdown occurs in the model when $R_2 \rightarrow 0$, leaving only the short along that path, and the inductance L and the negligible 1Ω resistor in the remainder of the circuit.

Thus, if the external impedance is properly matched to the spark inductance, switch closure will occur in the required $1/4$ ns. Therefore, the assumption that 1 cm SF_6 filled gaps at 100 atmospheres can be switched quickly enough and with enough synchronization becomes plausible. This is especially so considering the fact that the high pressures will improve matters according to the AFWL paper, if a sufficiently powerful UV laser is employed.

APPENDIX D

FINITE BASIS AXIAL DECOMPOSITION

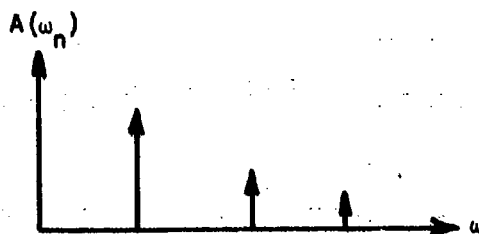
The frozen field distribution and distribution of the field ejected from a frozen field device are of finite extent. A basis consisting of all the sinusoidal functions that go to zero at the endpoints, and beyond, over such an interval is a convenient basis for the decomposition of such functions. An analogous situation using this basis is that of a finite string stretched between two fixed endpoints and displaced so that once released it will vibrate. The displaced case is exactly analogous to the frozen field configuration while the vibrating string, looking at one traveling wave making up the standing wave vibration, is exactly analogous to the behavior of the ejected wave.

The requirement that the sinusoidal functions be zero at the endpoints and beyond results in a discrete set of basis functions. A decomposition of some arbitrary function within the finite interval is thus given by a sum over these sinusoidal functions rather than an integral. The term with the lowest frequency is referred to as the fundamental or 1st harmonic. Higher terms have frequencies that are integral multiples of the fundamental's frequency and are referred to as harmonics (2nd, 3rd, etc.).

Another choice of basis functions that could have been employed, but was not, was that of sinusoidal functions of infinite extent. They form a continuous set of basis functions requiring an integral representation of the decomposition. Decomposing a waveform of finite extent in this basis gives a frequency distribution that, for example, looks like



as opposed to the decomposition in the discrete basis that looks like



While not true sine waves, the discrete basis is much simpler to use and the results are easily visualized. For the intervals encountered in this work, the difference between the finite extent sine wave decomposition and a decomposition using true sinusoids of infinite extent is small (i.e., the fraction of the total energy in a harmonic (finite basis) is nearly the same as that at and about the equivalent peak in the frequency distribution (infinite basis)).

UNCLASSIFIED

SECURITY CLASSIFICATION OF THIS PAGE (When Data Entered)

REPORT DOCUMENTATION PAGE		READ INSTRUCTIONS BEFORE COMPLETING FORM
1. REPORT NUMBER RADC-TR-74-111	2. GOVT ACCESSION NO.	3. RECIPIENT'S CATALOG NUMBER
4. TITLE (and Subtitle) CHEMICAL REACTION HERTZIAN GENERATOR	5. TYPE OF REPORT & PERIOD COVERED FINAL 31 May 73 to 30 Nov 73	
	6. PERFORMING ORG. REPORT NUMBER EDM/A-1-74-TR	
7. AUTHOR(s) Dr. K. S. Kunz	8. CONTRACT OR GRANT NUMBER(s) F30602-73-C-0318	
9. PERFORMING ORGANIZATION NAME AND ADDRESS Braddock, Dunn and McDonald, Inc. 1st Natl Bank Bldg, E Suite 1717 Albuquerque, NM 87108	10. PROGRAM ELEMENT, PROJECT, TASK AREA & WORK UNIT NUMBERS 55730644	
11. CONTROLLING OFFICE NAME AND ADDRESS Rome Air Development Center (OCTP) Griffiss AFB NY 13441	12. REPORT DATE May 1974	
	13. NUMBER OF PAGES 141	
14. MONITORING AGENCY NAME & ADDRESS (if different from Controlling Office) Same	15. SECURITY CLASS. (of this report) Unclassified	
	15a. DECLASSIFICATION/DOWNGRADING N/A SCHEDULE	
16. DISTRIBUTION STATEMENT (of this Report) Distribution limited to U.S. Government agencies only; Test and Evaluation; May 1974. Other requests for this document must be referred to RADC/OCTP, Griffiss AFB, NY 13441.		
17. DISTRIBUTION STATEMENT (of the abstract entered in Block 20, if different from Report) Same		
18. SUPPLEMENTARY NOTES RADC Project Engineer: Mr. William Quinn (OCTP)		
19. KEY WORDS (Continue on reverse side if necessary and identify by block number) Microwave Circuit Elements Microwave Transmitters Pulse Power Electromagnetic Waves		
20. ABSTRACT (Continue on reverse side if necessary and identify by block number) This effort represents a first attempt at combining the two separate technologies of explosive flux compression and Hertzian generation for the purpose of obtaining ultra-high energy pulses at microwave frequencies. A number of interesting concepts were ana- lyzed and three were selected by the contractor as most deserving of future attention. It is hoped that this report will stimulate fur- ther imaginative and creative thought in this direction leading		

DD FORM 1 JAN 73 1473

EDITION OF 1 NOV 68 IS OBSOLETE

UNCLASSIFIED

SECURITY CLASSIFICATION OF THIS PAGE (When Data Entered)

UNCLASSIFIED

SECURITY CLASSIFICATION OF THIS PAGE(When Data Entered)

20.
eventually to a successful technique for accomplishing the
aforementioned goal.

UNCLASSIFIED

SECURITY CLASSIFICATION OF THIS PAGE(When Data Entered)